Synthesis of amide-linked phospholipids and their bilayer characterization

2022, March

Biological Science and Technology, Life and Materials Systems Engineering,

Graduate School of Advanced Technology and Science, Tokushima University

Toshiki NAKAO

Contents

Chapter 1.

General Introduction

Biological membranes are thin layered structures composed of extrinsic and integral membrane proteins incorporated in lipid bilayer membranes. They provide boundary regions of cell membranes and intracellular organelle membranes and play an essential role in maintaining life activities such as regulation of selective permeability of substances and reaction fields of signal transduction [1, 2].

The study of biological membranes was begun in 1925 by Gorter and Grendel, who proved that biological membranes are constituted by lipid bilayer membranes. They found that the area of extracted phospholipids from an erythrocyte is twice as large as that of a membrane of the erythrocyte spread as a single layer on water surface [3]. Then, Daniel and Davson proposed a sandwich model containing a phospholipid layer between protein layers in 1935 [4]. They explained that the hydrophobic region of phospholipid membranes is apart from an aqueous solution and the hydrophilic region is in contact with water, and proteins cover the surface of phospholipid bilayer membranes. In 1972, Singer and Nicolson established a “fluid mosaic model” that is accepted as membrane structures at present [5]. This model described that proteins are partially or entirely embedded in a phospholipid bilayer membrane. Fluid mosaic model of biological membranes has developed to concept of lipid raft, which is a specific domain formed in biological membranes proposed by Simons and Ikonen in the late 1990’s [6-8]. This lipid raft consists of sphingophospholipids with saturated acyl chains and cholesterol, and it is supposed that the region does not mix peripheral bilayer regions of

glycerophospholipids with unsaturated acyl chains and forms micro domains segregated laterally in the membranes.

Lipids are amphipathic substances having hydrophobic groups such as fatty-acid chains and a polar head group consisting of various functional groups. Phospholipids found in biological membranes of eukaryotes comprise a lot of glycerophospholipids and a few sphingophospholipids [9]. The molecular backbones of these lipids are a glycerol for the former lipids and an amino alcohol named as a sphingosine for the latter lipids, respectively. The major difference between the two lipids is in the linkage type of the hydrophobic chains to the backbone. In glycerophospholipids, two long-chain fatty acids bind to the backbone by an ester linkage, whereas in sphingophospholipids, one hydrophobic chain is a long-chain alcohol contained in the backbone while another one is a long-chain fatty acid bound by an amide linkage to the amino group on the side chain.

The author takes up a glycero- and sphingo- mixed type phospholipid, which has the two fatty acids bind to the backbone by an amide linkage, as an analog of sphingomyelin in this study. This mixed type of phospholipid has been first investigated by Sunamoto, et al. in the early 1990's [10-12]. They have synthesized the amide-linked PC with two myristoyl chains to study a complex of membrane proteins and boundary lipids in the surroundings, which is the so-called current lipid raft consisted of GPI-anchored proteins and sphingophospholipids. They have also reported the bilayer properties [10, 13, 14]. In the 2000's, a group of Zumbuehl et al. [15-20] in Switzerland have synthesized the amide-linked PC with two palmitoyl chains and several positional isomers with different chain lengths and reported their bilayer properties. Interestingly, they have observed that some amide-linked PCs form cubic vesicles rather than spherical vesicles at low temperatures [18, 19]. However, the phase behavior of these amide-linkage PCs has not yet been explained in detail, though fundamental structural properties

(e.g., bilayer repeat distance) have been obtained.

Outline of This Thesis

On the basis of the above research background, the author decided to investigate bilayer properties of unnatural phospholipids with amide linkages in the molecular backbone. Chapter 2 describes the organic syntheses of amide-linked PCs. Taking account of the previous studies, the author chose the four kinds of racemic forms of amide-linked PCs containing linear saturated alkyl chain and the two kinds of the *R* forms of optical isomers. Chapter 3 compare the effect of the difference in linkage type of hydrophobic chains on the bilayer properties. Here, the author selected dipalmitoylamidodeoxyphosphatidylcholine (DPADPC) for this purpose. The phase transitions of the DPADPC bilayer membrane are observed under atmospheric and high pressure. The obtained thermal phase behavior, *T*–*p* phase diagram and phase-transition quantities of the DPADPC bilayer membrane are compared with the corresponding results of the linkage isomers, ester- and ether-linked PCs. Furthermore, the motility of the lipid molecule in these bilayer membranes under atmospheric pressure is also discussed. By using these results, the author considers the effect of the difference in chain-linkage type of the PC molecule on the above bilayer properties. Finally, the conclusions of this study are summarized comprehensively, and the future perspective is described, in Chapter 4.

Chapter 2.

Synthesis of amide-linked phospholipids

2.1. Introduction

Studies of lipid bilayer membranes are mostly made on natural lipids such as glycerophospholipids and sphingophospholipids. Accordingly, when we use unnatural lipids for experimental purpose, we have to synthesize the lipids except for commercially available ones. Although it is hard to synthesize such lipids in general due to the difficulty of selection of appropriate solvent for the synthesis and purification and the unavailability of conventional synthetic techniques such as liquid/liquid extraction, we can now fortunately refer to a large number of literatures on syntheses of natural and unnatural phospholipids.

In this study, the author selected amide-linked unnatural phospholipids, focusing on how the difference in linkage type affects phase behavior and membrane properties of phospholipids, in order to compare the results with those of linkage isomers of natural phospholipids such as ester-linked and ether-linked ones. At first, a racemic amide-linked phospholipid with saturated long fatty-acid (palmitoyl) chains, 1,2-*rac*-dipalmitoylamido-1,2-deoxyphosphatidylcholine (DPADPC) was synthesized. Next, a series of hydrophobic-chain homologs of DPADPC, 1,2-*rac*-dilauroylamido-1,2-deoxyphosphatidylcholine (DLADPC), 1,2-*rac*-dimyristoylamido-1,2-deoxyphosphatidylcholine (DMADPC), and 1,2-*rac*-distearoylamido-1,2-

deoxyphosphatidylcholine (DSADPC) were synthesized. Since glycerophospholipids have a glycerol backbone including an asymmetric carbon atom, there are two kinds of optical isomers, *R* and *S* forms. Here, the author selected the optical isomer (*R*-form) of DPADPC and DMADPC and subsequently synthesized (*R*)-(-)-1,2-dipalmitoylamido-1,2-deoxyphosphatidylcholine and (*R*)-(-)-1,2-dimyristoylamido-1,2-deoxyphosphatidylcholine.

The variable modular structure of a lipid molecule is the source of the diversity of phospholipids though, the manner of arrangement between each module such as types of linkage between hydrophobic chains and backbone and order of modules in the molecule is common to most membrane lipids. Therefore, it is expected that the investigation of correlation between module-modified unnatural phospholipids and the bilayer phase behavior will provide fundamental information on the intrinsic significance and roles of membrane lipids.

2.2. General Information

All chemical reagents were obtained from Tokyo Chemical Industry Co., Ltd. (Tokyo, Japan). 2 M HCl/methanol solution was obtained from Kokusan Chemical Co., Ltd. (Tokyo, Japan) and other solvents were obtained from Kanto Chemical Co., Inc. (Tokyo, Japan). Thin-layer chromatography was performed on silica gel (Silica Gel 60) purchased from Merck KGaA, (Tokyo, Japan). Column chromatography was performed on silica gel (60N: spherical, neutral, 63-210 μm) purchased from Kanto Chemical Co., Inc. Ion exchange resin (Amberlite MB-20) obtained from Merck KGaA was used.

^{1}H-NMR spectra of lipid samples were recorded in $CDCl_3$, CD_3OD or D_2O using tetramethyl silane as the internal standard by a JNM-ECZ-400S NMR spectrometer of 400 MHz (JOEL, Ltd, Tokyo, Japan). Spectra of liquid chromatography – mass spectrometry (LC-MS) were measured by an UPLC-MS apparatus (Waters, Corp. Tokyo, Japan).

2.3. Synthesis of 1,2-*rac*-dipalmitoylamido-1,2-deoxyphosphatidylcholine (DPADPC)

The synthetic procedure of DPADPC is given as the following together with the scheme (Figure. 1) and available elsewhere [21, 22].

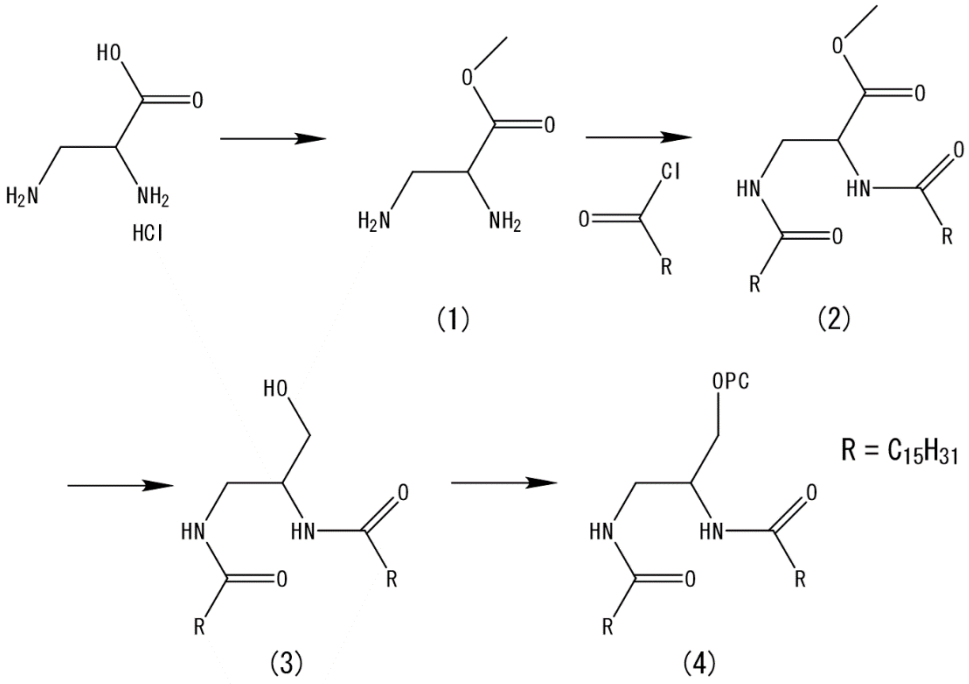

Figure. 1. Synthetic scheme of DPADPC

2.3.1. Methyl 2,3-diaminopropionate (1):

1.0 g (7.1 mmol) of DL-2,3-diaminopropinic acid monohydrochloride was dissolved in 100 ml of 2 M HCl/methanol solution. The mixture was refluxed at 90 °C for 17 h. The solvent was removed under reduced pressure to give 1.60 g as a yellow viscous oil of 80-90 % purity depending on the batch.

^{1}H-NMR (400 MHz, D_2O): δ = 3.46 (m, 2H); 3.76 (s, 3H); 4.40 (m, 1H).

2.3.2. Methyl 2,3-dipalmitoylamidopropionate (2):

1.6 g (7.1 mmol) of (1) was added to 10 ml (72.1 mmol) of triethylamine and 90 ml of dry DMF and immediately followed by a dropwise addition of 8 ml (26.5 mmol) of palmitoyl chloride. The mixture was stirred at 65 °C for 6 h. The reaction product was filtered to remove triethylamine hydrochloride and the filtrate was condensed. The obtained crude product was dissolved into dichloromethane and then washed by 1 M HCl once and a saturated N_aHCO_3 solution once. The organic layer collected was dried with $MgSO_4$ and concentrated under reduced pressure. The dried product was recrystallization from methanol to give (2), where the yield was 2.75 g (54.7 %).

^{1}H-NMR (400 MHz, $CHCl_3$): δ = 0.862 (m, 6H); 1.23 (s, 48H); 1.60 (m, 4H); 2.17 (m, 4H); 3.63 (m, 2H); 3.74 (s, 3H); 4.58 (br, 1H); 6.05 (m, 1H); 6.74 (m, 1H).

2.3.3. 1,2-Dipalmitoylamidopropan-3-ol (3):

2.75 g (4.6 mmol) of (2), 0.68 g (17 mmol) of sodium borohydride and 0.85 g (41 mmol) of lithium chloride were mixed in 40 ml of dry ethanol and reacted at 60 °C for 4 h for hydrogenation. The reaction product was condensed to remove the solvent. The obtained crude product was dissolved in dichloromethane and then washed by 1 M HCl once and a saturated N_aHCO_3 solution once. The organic layer collected was dried with $MgSO_4$ and concentrated under reduced pressure. The dried product was recrystallization from ethanol to give (3), where the yield was 2.23 g (85.4 %).

^{1}H-NMR (400 MHz, $CDCl_3$): δ = 0.88 (m, 6H); 1.24 (s, 48H); 1.58 (m, 4H); 2.20 (m, 4H); 3.23 (m, 1H); 3.51 (m, 2H); 3.65 (m, 1H); 3.85 (m, 1H); 6.11 (m, 1H); 6.27 (m, 1H).

2.3.4. 1,2-rac-Dipalmitoylamido-1,2-deoxyphosphatidylcholine (4):

4.28 g (7.55 mmol) of (3), 3.0 ml (17 mmol) of *N*,*N*-diisopropylethylamine, and 0.57 g of *N*,*N*-dimethyl-4-aminopyridine were mixed in 80 ml of dry dichloromethane. Then 4.0 ml (31 mmol) of 2-chloro-1,3,2- dioxaphospholane was added to the mixture and was stirred for 24h at 0 °C, and subsequently 3 ml (58 mmol) of bromine was added. After 15 min at 0 °C, the solvent was removed under reduced pressure. The obtained product was dissolved in 78 ml of a mixed solution of chloroform/2-propanol/acetonitrile (volume ratio of 3:5:5) and 56 ml of 30 % aqueous trimethylamine solution was added. After 72 h at room temperature, all the solvents were removed and the crude product was suspended in water. The suspension was centrifuged at 4 °C three times (10,000 rpm, 10 min) and dried under reduced pressure. The crude product was dissolved in a minimum amount of a chloroform/methanol (volume ratio of 1:1) solution and reprecipitated with 20-fold volumes of acetone. The precipitate was dissolved a minimum amount of a tetrahydrofuran/water (volume ratio of 9:1) solution and passed through an Amberlite MB-20 ion exchange column. Fractions containing product (4) were collected and it was purified by column chromatography on silica gel (elute solution: chloroform/methanol/water (volume ratio of 65:25:4)) to give (4) as a white solid, where the yield was 1.73 g (31 %).

Anal.: calc. for $C_{40}H_{83}N_3O_6P \cdot 4H_2O$, C 59.75; H 11.28; N 5.23 %, found: C 59.81; H 10.88; N 5.20 %. ^{1}H-NMR (400 MHz, $CDCl_3$/CD_3OD (1:1) with TMS): δ = 0.89 (m, 6H); 1.28 (s, 48H); 1.59 (m, 4H); 2.17 (m, 4H); 3.22 (s, 9H); 3.33-3.41 (m, 2H); 3.63 (m, 2H); 3.87 (m, 2H); 4.14 (m, 1H); 4.28 (m, 2H); 7.88 (m, 1H); 7.99 (m, 1H). ^{13}C-NMR ($CDCl_3$/CD_3OD (1:1)): δ = 175.9, 175.0, 66.1, 64.7, 59.3, 53.8, 49.8, 39.9, 36.7, 31.7, 30.3, 29.3, 25.8, 23.3, 22.7, 13.7. ^{31}P-NMR ($CDCl_3$/CD_3OD (1:1)): δ = -0.1. LC-MS (ESI+) *m/z* calc. $[M+H]^+$ 732.6019; obs. 732.6021.

2.4. Synthesis of 1,2-*rac*-dilauroylamido-1,2-deoxyphosphatidylcholine (DLADPC)

2.4.1. Methyl 2,3-dilauroylamidopropionate (5):

3.2 g (16.8 mmol) of (1) was added to 20 ml (0.14 mol) of triethylamine and 150 ml of dry DMF and immediately followed by a dropwise addition of 14 ml (58.9 mmol) of lauroyl chloride. The mixture was stirred at 65 °C for 6 h. The reaction product was filtered to remove triethylamine hydrochloride and the filtrate was condensed. The obtained crude product was dissolved into dichloromethane and then washed by 1 M HCl once and a saturated N_aHCO_3 solution once. The organic layer collected was dried with $MgSO_4$ and concentrated under reduced pressure. The dried product was recrystallization from methanol to give (5). (5) was moved forward with no further purification.

2.4.2. 1,2-Dilauroylamidopropan-3-ol (6):

3.57 g (7.4 mmol) of (5), 1.25 g (33 mmol) of sodium borohydride and 1.52 g (73 mmol) of lithium chloride were mixed in dry ethanol and stirred at 60 °C for 4 h for the hydrogenation reaction. The reaction product was filtered and the filtrate was condensed to remove ethanol. The obtained crude product was dissolved in dichloromethane and then washed by 1 M HCl once and a saturated N_aHCO_3 solution once. The organic layer collected was dried with $MgSO_4$ and concentrated under reduced pressure. The dried product was recrystallization from ethanol to give (6). (6) was moved forward with no further purification.

2.4.3. 1,2-rac-Dilauroylamido-1,2-deoxyphosphatidylcholine (7):

2.59 g (5.7 mmol) of (6) and 3.0 ml (17 mmol) of *N*,*N*-diisopropylethylamine were mixed in 100 ml of dry dichloromethane. Then 3.5 ml (28 mmol) of 2-chloro-1,3,2-dioxaphospholane was added to the mixture and was stirred for 24h at 0 °C, and subsequently 3 ml (58 mmol) of bromine was added. After 15 min at 0 °C, the solvent was removed under reduced pressure. The obtained product was dissolved in 78 ml of a mixed solution of chloroform/2-propanol/acetonitrile (volume ratio of 3:5:5) and 56 ml of 30 % aqueous trimethylamine solution was added. After 72 h at room temperature, all the solvents were removed and the crude product was suspended in water. The suspension was centrifuged at 4 °C three times (10,000 rpm, 10 min) and dried under reduced pressure. The crude product was dissolved a minimum amount of a tetrahydrofuran/water (volume ratio of 9:1) solution and passed through an Amberlite MB-20 ion exchange column. Fractions containing product (7) were collected and it was purified by column chromatography on silica gel (elute solution: chloroform/methanol/water (volume ratio of 65:25:4)) to give (7) as a white solid, where the yield was 98 mg (28 %).

Anal.: calc. for $C_{32}H_{66}N_3O_6P{\cdot}5H_2O$, C 54.14; H 10.79; N 5.92 %, found: C 54.07; H 10.41; N 5.89 %. ^{1}H-NMR (400 MHz, $CDCl_3/CD_3OD$ (1:1) with TMS): δ = 0.89 (m, 6H); 1.28 (s, 32H); 1.59 (m, 4H); 2.17 (m, 4H); 3.22 (s, 9H); 3.41 (m, 2H); 3.63 (m, 2H); 3.87 (m, 2H); 4.14 (m, 1H); 4.28 (m, 2H); 7.88 (t, 1H); 7.99 (d, 1H). ^{31}P-NMR ($CDCl_3$): δ = -0.1. LC-MS (ESI+) *m/z* calc. $[M+H]^+$ 620.4767; obs. 620.4751.

2.5. Synthesis of 1,2-*rac*-dimyristoylamido-1,2-deoxyphosphatidylcholine (DMADPC)

2.5.1. Methyl 2,3-dimyristoylamidopropionate (8):

3.2 g (16.8 mmol) of (1) was added to 20 ml (0.14 mol) of triethylamine and 100 ml of dry DMF and immediately followed by a dropwise addition of 14 ml (51 mmol) of myristoyl chloride. The mixture was stirred at 65 °C for 6 h. The reaction product was filtered to remove triethylamine hydrochloride and the filtrate was condensed. The obtained crude product was dissolved into dichloromethane and then washed by 1 M HCl once and a saturated N_aHCO_3 solution once. The organic layer collected was dried with $MgSO_4$ and concentrated under reduced pressure. The dried product was recrystallization from methanol to give (8). (8) was moved forward with no further purification.

2.5.2. 1,2-Dimyristoylamidopropan-3-ol (9):

7.1 g (13 mmol) of (8), 2.5 g (0.11 mol) of sodium borohydride and 3.1 g (0.15 mol) of lithium chloride were mixed in dry ethanol and stirred at 60 °C for 4 h for the hydrogenation reaction. The reaction product was filtered and the filtrate was condensed to remove ethanol. The obtained crude product was dissolved in dichloromethane and then washed by 1 M HCl once and a saturated N_aHCO_3 solution once. The organic layer collected was dried with $MgSO_4$ and concentrated under reduced pressure. The dried product was recrystallization from ethanol to give (9). (9) was moved forward with no further purification.

2.5.3. 1,2-rac-Dimyristoylamido-1,2-deoxyphosphatidylcholine (10):

4.8 g (9.4 mmol) of (9) and 3.0 ml (17 mmol) of *N*,*N*-diisopropylethylamine were mixed in 80 ml of dry dichloromethane. Then 4.0 ml (31 mmol) of 2-chloro-1,3,2-dioxaphospholane was added to the mixture and was stirred for 24h at 0 °C, and subsequently 3 ml (58 mmol) of bromine was added. After 15 min at 0 °C, the solvent was removed under reduced pressure. The obtained product was dissolved in 78 ml of a mixed solution of chloroform/2-propanol/acetonitrile (volume ratio of 3:5:5) and 56 ml of 30 % aqueous trimethylamine solution was added. After 72 h at room temperature, all the solvents were removed and the crude product was suspended in water. The suspension was centrifuged at 4 °C three times (10,000 rpm, 10 min) and dried under reduced pressure. The crude product was dissolved in a minimum amount of a chloroform/methanol (volume ratio of 1:1) solution and reprecipitated with 20-fold volumes of acetone. The precipitate was dissolved a minimum amount of a tetrahydrofuran/water (volume ratio of 9:1) solution and passed through an Amberlite MB-20 ion exchange column. Fractions containing product (10) were collected and it was purified by column chromatography on silica gel (elute solution: chloroform/methanol/water (volume ratio of 65:25:4)) to give (10) as a white solid, where the yield was 0.91 g (14 %).

Anal.: calc. for $C_{36}H_{74}N_3O_6P{\cdot}2H_2O$, C 60.73; H 11.04; N 5.90 %, found: C 60.64; H 11.03; N 6.01 %. ^{1}H-NMR (400 MHz, $CDCl_3/CD_3OD$ (1:1) with TMS): δ = 0.89 (m, 6H); 1.28 (s, 40H); 1.59 (m, 4H); 2.17 (m, 4H); 3.22 (s, 9H); 3.41 (m, 2H); 3.63 (m, 2H); 3.87 (m, 2H); 4.14 (m, 1H); 4.28 (m, 2H); 7.88 (t, 1H); 7.99 (d, 1H). ^{31}P-NMR ($CDCl_3$): δ = -0.1. LC-MS (ESI+) *m/z* calc. $[M+H]^+$ 676.5394; obs. 676.5424.

2.6. Synthesis of 1,2-*rac*-distearoylamido-1,2-deoxyphosphatidylcholine (DSADPC)

2.6.1. Methyl 2,3-distearoylamidopropionate (11):

3.2 g (16.8 mmol) of (1) was added to 20 ml (0.14 mol) of triethylamine and 150 ml of dry DMF and immediately followed by a dropwise addition of 17 ml (51 mmol) of stearoyl chloride. The mixture was stirred at 65 °C for 6 h. The reaction product was filtered to remove triethylamine hydrochloride and the filtrate was condensed. The obtained crude product was dissolved into dichloromethane and then washed by 1 M HCl once and a saturated N_aHCO_3 solution once. The organic layer collected was dried with $MgSO_4$ and concentrated under reduced pressure. The dried product was recrystallization from methanol to give (11). (11) was moved forward with no further purification.

2.6.2. 1,2-Distearoylamidopropan-3-ol (12):

6.1 g (9.4 mmol) of (11), 0.63 g (17 mmol) of lithium borohydride were mixed in dry tetrahydrofuran and stirred at 60 °C for 24 h for the hydrogenation reaction. The reaction product was filtered and the filtrate was condensed to remove tetrahydrofuran. The obtained crude product was dissolved in dichloromethane and then washed by 1 M HCl once and a saturated N_aHCO_3 solution once. The organic layer collected was dried with $MgSO_4$ and concentrated under reduced pressure. The dried product was recrystallization from ethanol to give (12). (12) was moved forward with no further purification.

2.6.3. 1,2-rac-Distearoylamido-1,2-deoxyphosphatidylcholine (13):

1.0 g (1.6 mmol) of (12) and 0.8 ml (5.7 mmol) of *N*,*N*-diisopropylethylamine were mixed in 100 ml of dry dichloromethane. Then 0.8 ml (6.3 mmol) of 2-chloro-1,3,2-dioxaphospholane was added to the mixture and was stirred for 24h at 0 °C, and subsequently 0.8 ml (5.0 mmol) of bromine was added. After 15 min at 0 °C, the solvent was removed under reduced pressure. The obtained product was dissolved in 78 ml of a mixed solution of chloroform/2-propanol/acetonitrile (volume ratio of 3:5:5) and 56 ml of 30 % aqueous trimethylamine solution was added. After 72 h at room temperature, all the solvents were removed and the crude product was suspended in water. The suspension was centrifuged at 4 °C three times (10,000 rpm, 10 min) and dried under reduced pressure. The crude product was dissolved in a minimum amount of a chloroform/methanol (volume ratio of 1:1) solution and reprecipitated with 20-fold volumes of acetone. The precipitate was dissolved a minimum amount of a tetrahydrofuran/water (volume ratio of 9:1) solution and passed through an Amberlite MB-20 ion exchange column. Fractions containing product (13) were collected and it was purified by column chromatography on silica gel (elute solution: chloroform/methanol/water (volume ratio of 65:25:4)) to give (13) as a white solid, where the yield was 240 mg (19 %).

Anal.: calc. for $C_{44}H_{90}N_3O_6P{\cdot}5H_2O$, C 60.17; H 11.48; N 4.78 %, found: C 60.51; H 11.00; N 4.66 %. ^{1}H-NMR (400 MHz, $CDCl_3/CD_3OD$ (1:1) with TMS): δ = 0.89 (m, 6H); 1.28 (s, 56H); 1.59 (m, 4H); 2.17 (m, 4H); 3.22 (s, 9H); 3.41 (m, 2H); 3.63 (m, 2H); 3.87 (m, 2H); 4.14 (m, 1H); 4.28 (m, 2H); 7.88 (t, 1H); 7.99 (d, 1H). ^{31}P-NMR ($CDCl_3$): δ = -0.1. LC-MS (ESI+) *m/z* calc. $[M+H]^+$ 788.6646; obs. 788.6672.

2.7. Synthesis of (*R*)-(-)-1,2-dipalmitoylamido-1,2-deoxyphosphatidylcholine (*R*-DPADPC)

2.7.1. (R)-(-)-Methyl 2,3-diaminopropionate (14):

2.0 g (14.2 mmol) of (*R*)-(-)-2,3-diaminopropinic acid monohydrochloride was dissolved in 50 ml of 2 M HCl/methanol solution. The mixture was refluxed at 90 °C for 6 h. The solvent was removed under reduced pressure to give 3.20 g as a yellow oil of 80-90 % purity depending on the batch.

^{1}H-NMR (400 MHz, D_2O): δ = 3.46 (d, 2H); 3.76 (s, 3H); 4.40 (m, 1H).

2.7.2. (R)-(-)-Methyl 2,3-dipalmitoylamidopropionate (15):

3.2 g (16.8 mmol) of (14) was added to 20 ml (0.14 mol) of triethylamine and 100 ml of dry DMF and immediately followed by a dropwise addition of 16 ml (53.0 mmol) of palmitoyl chloride. The mixture was stirred at 70 °C for 10 h. The reaction product was filtered to remove triethylamine hydrochloride and the filtrate was condensed. The obtained crude product was dissolved into dichloromethane and then washed by 1 M HCl once and a saturated N_aHCO_3 solution once. The organic layer collected and concentrated under reduced pressure. The dried product was recrystallization from methanol to give (15). (15) was moved forward with no further purification.

2.7.3. (R)-(-)-1,2-dipalmitoylamidopropan-3-ol (16):

8.32 g (14.0 mmol) of (15), 1.39 g (37 mmol) of sodium borohydride and 1.54 g (37 mmol) of lithium chloride were mixed in dry ethanol 100 ml and stirred at 60 °C for 4 h for the hydrogenation reaction. The reaction product was filtered and the filtrate was

condensed to remove ethanol. The obtained crude product was dissolved in dichloromethane and then washed by 1 M HCl once and a saturated N_aHCO_3 solution once. The organic layer collected and concentrated under reduced pressure. The dried product was recrystallization from ethanol to give (16). (16) was moved forward with no further purification.

2.7.4. (R)-(-)-1,2-dipalmitoylamido-1,2-deoxyphosphatidylcholine (17):

5.34 g (9.42 mmol) of (16) and 3.0 ml (17 mmol) of *N*,*N*-diisopropylethylamine and 0.52 g of DMAP were mixed in 100 ml of dry dichloromethane. Then 4.0 ml (32 mmol) of 2-chloro-1,3,2-dioxaphospholane was added to the mixture and was stirred for 24h at 0 °C, and subsequently 3 ml (58 mmol) of bromine was added. After 15 min at 0 °C, the solvent was removed under reduced pressure. The obtained product was dissolved in 78 ml of a mixed solution of chloroform/2-propanol/acetonitrile (volume ratio of 3:5:5) and 56 ml of 30 % aqueous trimethylamine solution was added. After 72 h at room temperature, all the solvents were removed and the crude product was suspended in water. The suspension was centrifuged at 4 °C three times (10,000 rpm, 10 min) and dried under reduced pressure. The crude product was dissolved a minimum amount of a tetrahydrofuran/water (volume ratio of 9:1) solution and passed through an Amberlite MB-20 ion exchange column. Fractions containing product (17) were collected and it was purified by column chromatography on silica gel (elute solution: chloroform/methanol/water (volume ratio of 65:25:4)) to give (17) as a white solid, where the yield was 924 mg (13 %).

Anal.: calc. for $C_{40}H_{83}N_3O_6P{\cdot}3.5H_2O$, C 60.42; H 11.28; N 5.28 %, found: C 60.48; H 10.87; N 5.33 %. ^{1}H-NMR (400 MHz, $CDCl_3/CD_3OD$ (1:1) with TMS): δ = 0.89 (m,

6H); 1.28 (s, 48H); 1.60 (m, 4H); 2.19 (m, 4H); 3.22 (s, 9H); 3.37-3.41 (m, 2H); 3.63 (m, 2H); 3.85-3.90 (m, 2H); 4.11 (m, 1H); 4.28 (m, 2H); 7.85 (m, 1H); 7.94 (m, 1H). ^{13}C-NMR (CDCl3/CD3OD (1:1)): δ = 175.5, 175.0, 66.1, 64.8, 59.2, 53.4, 49.7, 39.7, 36.0, 31.8, 29.5, 25.7, 22.4, 13.1. 31P-NMR (CDCl3/CD3OD (1:1)): δ = 0.4. LC-MS (ESI+) m/z calc. [M+H]+ 732.6019; obs. 732.6029.

2.8. Synthesis of (*R*)-(-)-1,2-dimyristoylamido-1,2-deoxyphosphatidylcholine (*R*-DMADPC)

2.8.1. (R)-(-)-Methyl 2,3-dimyristoylamidopropionate (18):

1.68 g (8.82 mmol) of (14) was added to 10 ml (0.70 mol) of triethylamine and 100 ml of dry DMF and immediately followed by a dropwise addition of 7 ml (25.5 mmol) of myristoyl chloride. The mixture was stirred at 65 °C for 6 h. The reaction product was filtered to remove triethylamine hydrochloride and the filtrate was condensed. The obtained crude product was dissolved into dichloromethane and then washed by 1 M HCl once and a saturated N_aHCO_3 solution once. The organic layer collected was dried with $MgSO_4$ and concentrated under reduced pressure. The dried product was recrystallization from methanol to give (18). (18) was moved forward with no further purification.

2.8.2. (R)-(-)-1,2-dimyristoylamidopropan-3-ol (19):

6.1 g (9.4 mmol) of (18), 0.63 g (17 mmol) of lithium borohydride were mixed in dry tetrahydrofuran and stirred at 60 °C for 24 h for the hydrogenation reaction. The reaction product was filtered and the filtrate was condensed to remove tetrahydrofuran. The obtained crude product was dissolved in dichloromethane and then washed by 1 M HCl once and a saturated N_aHCO_3 solution once. The organic layer collected was dried with $MgSO_4$ and concentrated under reduced pressure. The dried product was recrystallization from ethanol to give (19). (19) was moved forward with no further purification.

2.8.3. (R)-(-)-1,2-dimyristoylamido-1,2-deoxyphosphatidylcholine (20):

2.14 g (4.18 mmol) of (19) and 1.5 ml (8.5 mmol) of *N*,*N*-diisopropylethylamine were mixed in 80 ml of dry dichloromethane. Then 2.0 ml (15.5 mmol) of 2-chloro-1,3,2- dioxaphospholane was added to the mixture and was stirred for 24h at 0 °C, and subsequently 1.5 ml (29 mmol) of bromine was added. After 15 min at 0 °C, the solvent was removed under reduced pressure. The obtained product was dissolved in 78 ml of a mixed solution of chloroform/2-propanol/acetonitrile (volume ratio of 3:5:5) and 56 ml of 30 % aqueous trimethylamine solution was added. After 72 h at room temperature, all the solvents were removed and the crude product was suspended in water. The suspension was centrifuged at 4 °C three times (10,000 rpm, 10 min) and dried under reduced pressure. The crude product was dissolved in a minimum amount of a chloroform/methanol (volume ratio of 1:1) solution and reprecipitated with 20-fold volumes of acetone. The precipitate was dissolved a minimum amount of a tetrahydrofuran/water (volume ratio of 9:1) solution and passed through an Amberlite MB-20 ion exchange column. Fractions containing product (20) were collected and it was purified by column chromatography on silica gel (elute solution: chloroform/methanol/water (volume ratio of 65:25:4)) to give (20) as a white solid, where the yield was 0.63 g (22 %).

Anal.: calc. for $C_{36}H_{74}N_3O_6P{\cdot}4H_2O$, C 57.80; H 11.05; N 5.62 %, found: C 57.62; H 10.42; N 5.56 %. ^{1}H-NMR (400 MHz, $CDCl_3/CD_3OD$ (1:1) with TMS): δ = 0.89 (m, 6H); 1.27 (s, 40H); 1.60 (m, 4H); 2.20 (m, 4H); 3.24 (s, 9H); 3.42 (m, 2H); 3.64 (m, 2H); 3.86 -3.94(m, 2H); 4.10 (m, 1H); 4.30 (m, 2H); 7.87 (m, 1H); 8.08 (m, 1H). ^{31}P-NMR ($CDCl_3$): δ = 0.15. LC-MS (ESI+) *m/z* calc. $[M+H]^+$ 676.5394; obs. 676.5409.

Chapter 3.

Bilayer properties of an amide-linked phosphatidylcholine

3.1. Introduction

So far, author's research group has clarified states of bilayers formed by natural phospholipids by use of the temperature (T) – pressure (p) phase diagrams and thermodynamic quantities associated with the phase transitions [23-26]. On the other hand, there is little information available to answer the intrinsic question why phospholipids take such molecular structures. For example, if one of the linkage types at the glycerol backbone of a glycerophospholipid substitutes an amide linkage for an ester linkage, the molecular structure of a phospholipid will be similar to that of a sphingophospholipid. However, actually, there are no such phospholipids in nature and the amide linkage is introduced only in sphingophospholipids, which adopt more complex backbone structure (i.e., sphingosine). In order to reveal this sort of fundamental question for lipid molecular structure, it is useful to compare the bilayer properties of phospholipids which are mutually different only in the linkage type of hydrophobic chains to the backbone.

In our previous studies on bilayer phase transitions of phospholipids [27, 28], author's research group has found that bilayer phase behavior of ester-linked PCs, contained in biological membranes of eukaryotes, is markedly different from that of ether-linked PCs, contained in membranes of some extremophiles. The former PC lipids have

two acyl chains, each of which is bound to the glycerol backbone by an ester linkage, while the latter have two alkyl chains, each of which is bound to the glycerol backbone by an ether linkage. Hence, it is interesting to compare the bilayer properties of the amide-linked PC with those of the ester- and ether-linked PCs. Further, it is expected that the comparison provides us the fundamental information with respect to the difference in bilayer properties between glycerol- and sphingo-phospholipid.

In the present study, one of unnatural amide-linked PCs, DPADPC, which was made by a method of organic synthesis and purified it in Chapter 2, was selected for this purpose. And then, the phase transitions of the DPADPC bilayer membrane prepared were observed by differential scanning calorimetry (DSC) and high-pressure light transmittance measurement on DPADPC bilayer membrane. The resulting thermal behavior, *T–p* phase diagram and phase-transition quantities of the DPADPC bilayer membrane are compared with the corresponding results of linkage isomers (ester-linked isomer: dipalmitoylphosphatidylcholine (DPPC) and ether-linked isomer: dihexadecylphophatidylcholine (DHPC)). Furthermore, the motility of the lipid molecule in these bilayers is evaluated from nuclear magnetic resonance (NMR) measurement under atmospheric pressure. Based on these results, the effect of the difference in linkage type of hydrophobic chains on the bilayer properties is discussed.

3.2. Experimental

3.2.1. Materials and sample preparation:

An unnatural amide-linked phospholipid, 1,2-*rac*-diamido-1,2-deoxyphosphatidylcholine was obtained by a method of organic synthesis method and used after purification. The synthetic procedure is described in Chapter 2.1 with Figure 1. Two synthetic phospholipids, 1,2-dipalmitoyl-*sn*-glycero-3-phosphocholine and 1,2-di-*O*-hexadecyl-sn-glycero-3-phosphocholine, were purchased from Avanti Polar Lipids Inc. (Alabaster, AL). They were used without further purification. The molecular structures of three phosphatidylcholines used in this study are shown in Figure 2. Water purified by an ultrafiltration apparatus was used for sample preparation.

The multilamellar vesicle (MLV) solutions of DPADPC were prepared by suspending the lipid in water using a vortex mixer at concentrations of 1.0 mmol kg^{-1} for DSC and light-transmittance measurements. The DPADPC suspensions were sonicated for a few minutes by using a sonicator (Branson Digital Sonifier S-450D) at a temperature several degrees above the main-transition temperature of the bilayer membrane. In the NMR measurements, the MLV or stacked bilayer solutions of three kinds of PCs were prepared by suspending each lipid in solvent water (900 μl pure water and 100 μl deuterium oxide) at a concentration of 100 mM (ca. 7 wt %). Here deuterium oxide was used to fix the signal in the measurements. The prepared suspensions were sonicated for 30 minutes by using the sonicator at about 80 °C before measurements.

A thermal pretreatment called dynamic and static annealing was performed to form a L_c phase that is the most stable phase at a low temperature. The treatment enables us to promote the formation of the L_c phase by changing binding mode of water near the

polar head group of a lipid molecule in the bilayer membrane [29, 30]. In the dynamic annealing, freeze and thaw cycles at a low temperature were repeated for DPADPC samples until the constant enthalpy values were obtained for the transition related to the hydrated crystalline phase. Here, 1 thermal cycle comprises freezing storage at –15°C for 23 hour, and at –30°C for 1 hour and cold storage at 5°C for one day taking account of the freezing behavior of interlamellar water around the polar head group of a PC molecule [31, 32]. On the other hand, in the static annealing, DPADPC samples were allowed to stand for 24 hours at high temperatures (27 °C, 37 °C and 40.8 °C) around the main-transition temperature, respectively, before measurements.

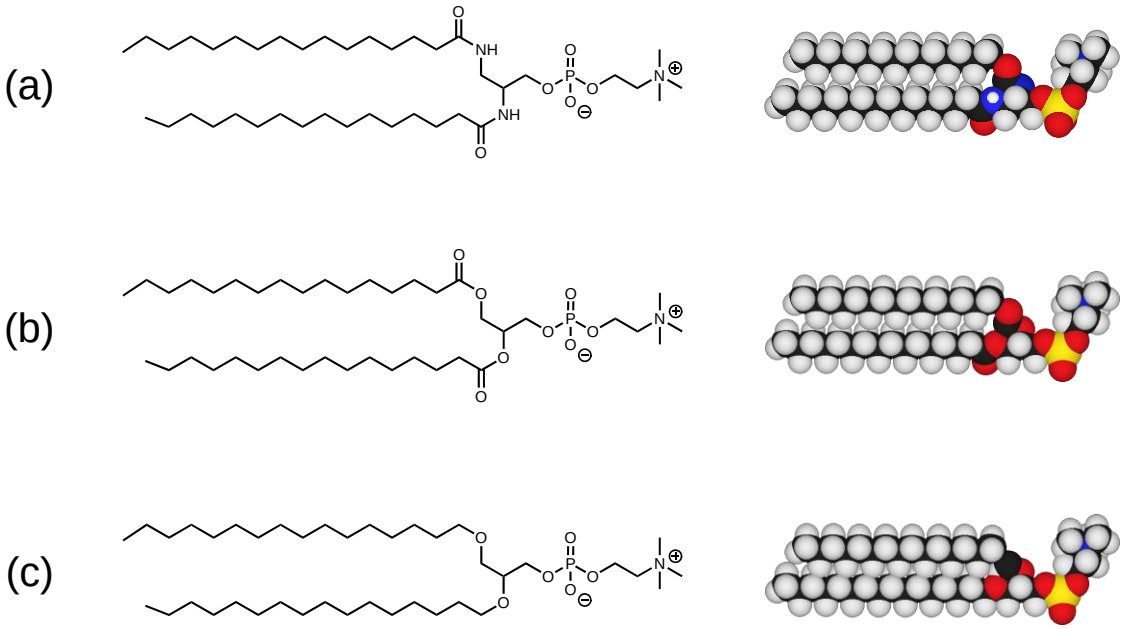

Figure. 2. Molecular structures of phospholipids with different hydrophobic linkages. (a) DPADPC, (b) DPPC, (c) DHPC.

3.2.2. DSC measurements:

The phase transitions of DPADPC multilamellar vesicles under atmospheric pressure were observed by a high-sensitivity differential scanning calorimeter, VP-DSC (Malvern Instrum. Ltd., Worcestershire, UK). After a degas treatment of 10 min for sample and reference solutions, the measurements were carried out under a heating (or cooling) rate of 0.75 K min^{-1} in the temperature range within 10 – 60 °C. The obtained thermal data were analyzed by software Origin 8.1 (Lightstone Corp., Tokyo, Japan).

3.2.3. Light-transmittance measurements:

The phase transitions of DPADPC multilamellar vesicles under high pressure were observed by an U-3010 spectrophotometer (Hitachi High-Technology Corp., Tokyo, Japan) with a high-pressure cell assembly PCI-400 (Syn. Corp., Kyoto, Japan). The isobaric thermotropic measurements were performed by a temperature scanning method at constant pressure. After injecting the sample solution into a drum quartz cell (2 ml), a cylindrical quartz cell (2 ml) or a micro quartz cell (200 μl), the cell was mounted in the assembly. Thermostated water from a programable water bath (TAITEC EZL-80F) was circulated through a jacket enclosing the cell and maintained for thermal equilibrium at the starting temperature for about 10 minutes. Abrupt changes in transmittance of monochromic light at the wavelength of 560 nm with increasing temperature (heating rate: 0.33 and 0.5 K min^{-1}) were observed and the phase-transition temperatures and pressure were determined. Pressures were generated by a hand-operated HP-500 hydraulic pump (Syn. Corp., Kyoto, Japan) and monitored using a Heise gauge with an accuracy of 0.2 MPa. Ligroin was used as a pressure medium. Further detailed procedures for the light transmittance measurements were described elsewhere [27, 33].

3.2.4. NMR measurements:

Samples for NMR measurements were resonicated for about 10 minutes to prevent the precipitation before measurements and then filled in NMR tubes with diameter of 5 mm. ^{13}C-NMR spectra of three kinds of PC bilayer membranes were measured as a function of temperature under the conditions of single pulse dec mode and integration times of 1000-2000 times by a JNM-ECA500 (JEOL Ltd., Tokyo, Japan). The obtained spectra were analyzed by attached software Delta ver.5.0.5.

3.3. Results and Discussion

3.3.1. Thermal phase behavior of DPADPC bilayer membrane:

DSC heating thermograms of DPADPC bilayer membrane annealed dynamically are demonstrated in Figure 3. The thermograms showed a single large endothermic peak at 41.4 °C in the first heating scan (1st scan) and a broad exothermic peak near 34 °C and a single large endothermic peak at 40.6 °C in second heating scan (2nd scan) where the sample is cooled down and reheated immediately after the first scan. For solids of lipids like triglycerides, although it sometimes happens that an exothermic peak is observed in the heating scan, which is called melt-mediated transformation [34]. This suggests that one polymorph of lipid with low stability melts and then another polymorph with high stability crystallizes in the heating process consecutively. Polymorphism of phases or forms is one of characteristics for lipids. But it has been hardly reported that such an exothermic peak is observed in the heating scan of lipid bilayer membrane. The present DSC results indicate that membrane lipids as well as lipids like oils and fats undergo such a phase transition between polymorphs. It seems that the exothermic peak observed in the 2nd scan is originated from the formation of a phase with high-ordered molecular structure due to the reorientation of DPADPC molecules in the bilayer membrane.

Since the difference in temperature between the endothermic peak in the 1st and 2nd scan is about 1 °C in the DSC measurements with low-temperature annealing, there is a possibility that the author observes the same phase transitions in both scans within experimental errors. Then, in order to clarify kinds of transitions of the two endothermic peaks, a high-temperature static annealing was performed at three temperatures (27.0 °C, 37.0 °C, 40.8 °C) in the vicinity of the phase-transition temperatures. This is because

low-temperature storage generally produces the most stable phase but a heat treatment near the transition temperatures can make the phase form faster when two transition temperatures are close to each other. Resulting thermograms are shown in Figure 4. For the DPADPC bilayer membrane treated at 27.0 °C, the author observed only one large endothermic peak at 40.9 °C in the 1st scan while a broad exothermic peak near 34 °C and a large endothermic peak at 40.5 °C in the 2nd scan, which were almost the same results as those obtained by low-temperature annealing. By contrast, at 37.0 °C, the author observed a broad exothermic peak near 34 °C and a large endothermic peak at 40.4 °C accompanied with a shoulder peak at 42.6 °C in the 1st scan while a broad exothermic peak near 34 °C and a large endothermic peak at 40.4 °C in the 2nd scan, where the size of the endothermic peak in the 1st scan became smaller than that of the 2nd scan. At 40.8 °C, there was no change in peak appearance depending on the scan: a broad exothermic peak near 34 °C and a large endothermic peak at 40.5 °C was observed in both scans.

DSC cooling thermograms of DPADPC bilayer membrane obtained after the above 1st and 2nd heating scans are given in Figure 5. The thermogram after the 1st scan showed a single large exothermic peak at 39.0 °C. The author observed almost the same thermal behavior for the thermogram after the 2nd scan: there was no endothermic peak corresponding to the exothermic peak observed in the heating scan. This fact suggests that the high-temperature phase transforms directly into the low-temperature phase without going through the intermediate phase with decreasing temperature.

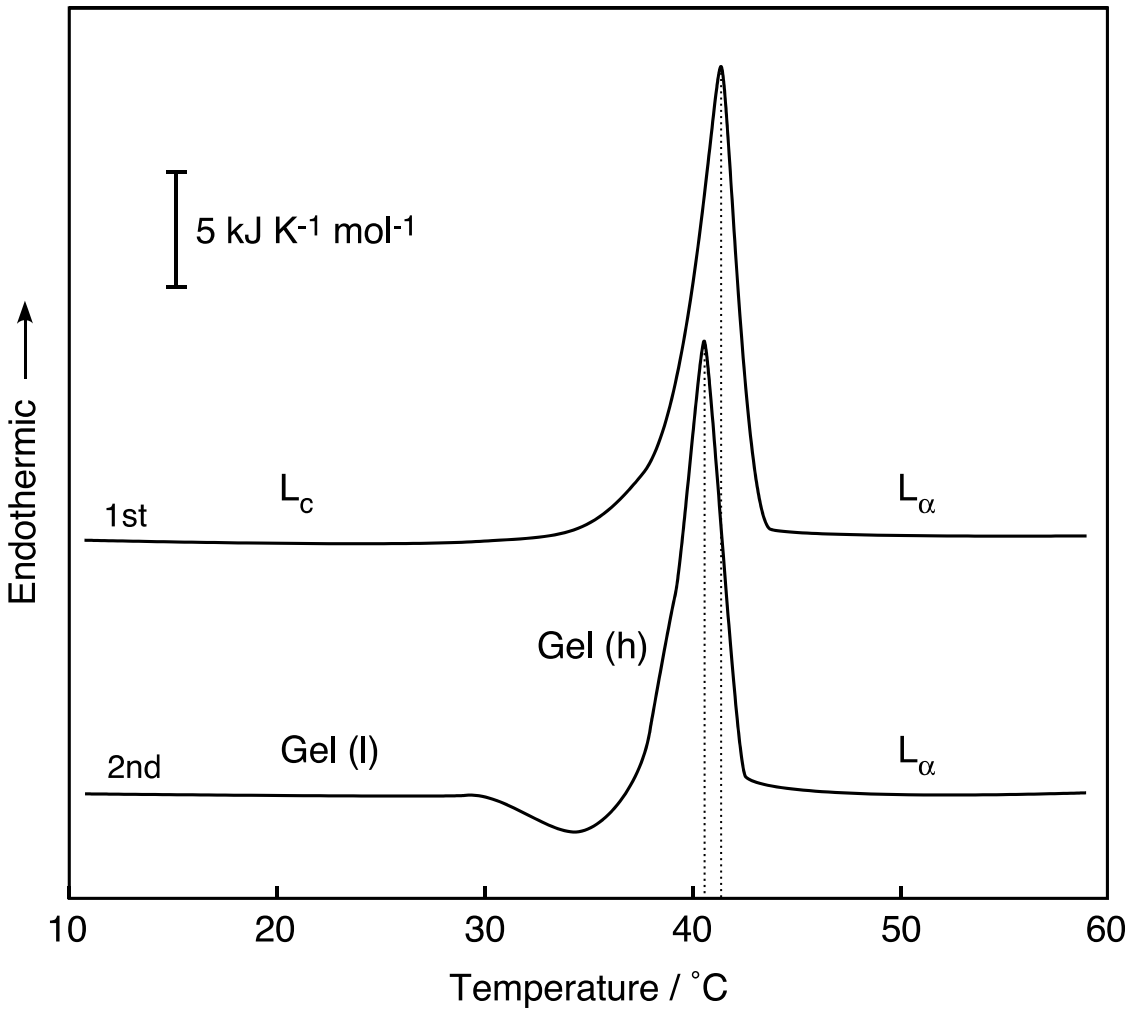

Figure. 3. DSC heating thermograms of DPADPC bilayer membrane annealed dynamically: (1) 1st scan, (2) 2nd scan. Here the annealing was repeated by 13 cycles. Dotted lines indicate the temperatures of endothermic peaks. Gel (l) and Gel (h) denote low-ordered and high-ordered gel phases, respectively.

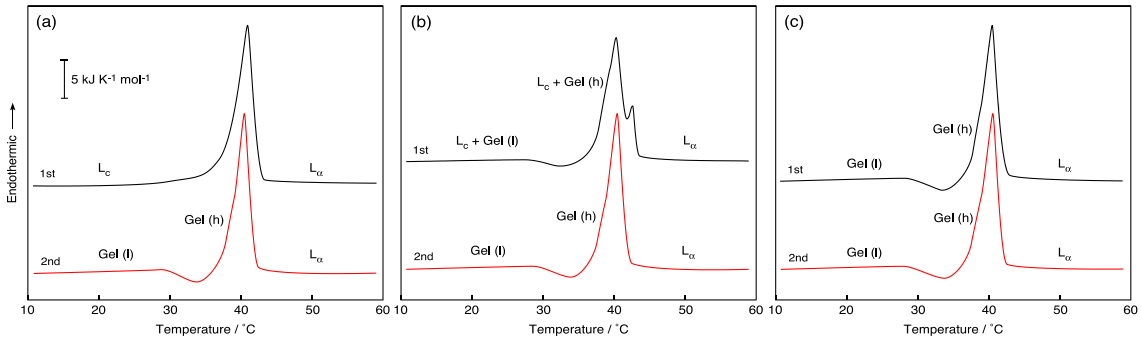

Figure. 4. DSC heating thermograms of DPADPC bilayer membrane annealed statically at various temperatures: (a) 27.0 °C, (b) 37.0 °C, (c) 40.8 °C; (1) 1st scan, (2) 2nd scan. Gel (l) and Gel (h) denote low-ordered and high-ordered gel phases, respectively.

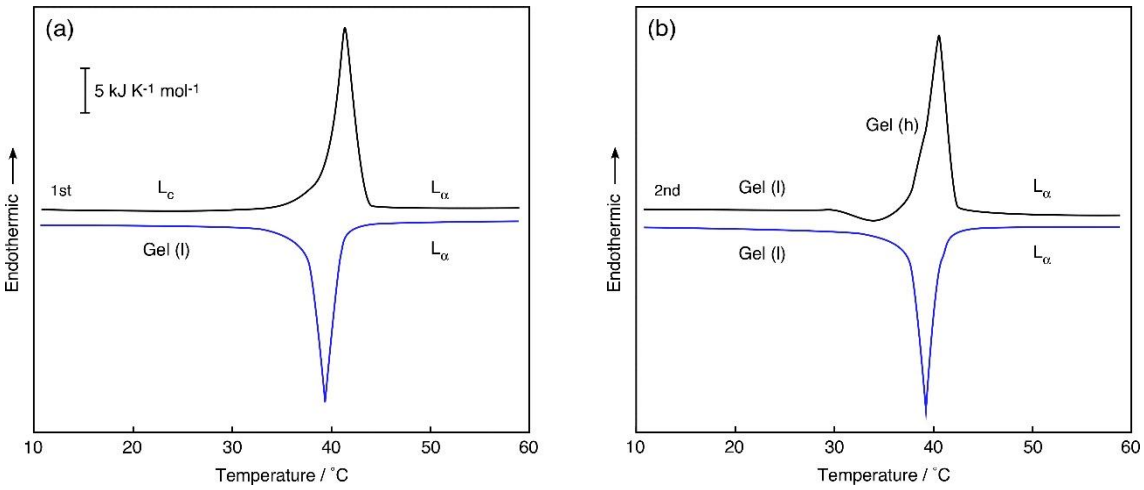

Figure. 5. DSC thermograms of DPADPC bilayer membrane: (a) 1st heating scan and the cooling scan, (b) 2nd heating scan and the cooling scan. Gel (l) and Gel (h) denote low-ordered and high-ordered gel phases, respectively. The temperature and transition enthalpy of the L_a/Gel (l) transition in the cooling scan are 39.0 °C and –30.5 kJ mol^{-1}, respectively.

Taking these results into consideration, the author identified the endothermic peak at 41.6 °C as the transition from the L_c phase to the liquid crystal (L_α) phase, the exothermic peak at about 34 °C as the transition from a low-ordered gel phase (Gel (l)) to the high-ordered gel phase (Gel (h)) and the endothermic peak at 40.4°C as the main transition from the Gel (h) phase to the L_α phase. Takahashi et al. have observed the similar phase behavior including an exothermic transition in a bilayer of amide-linked PC with two myristoyl-chains by X-ray diffraction and identified the gel phase in the high-temperature region as the highly ordered gel phase and showed that the lipid molecules in the highly ordered gel phase do not form an ordered two-dimensional lattice and the molecular packing is relatively disordered in comparison with the L_c phase of ester-linked PC bilayer membranes although the structures of both bilayer membranes in the gel (low-ordered) and L_α phases are almost the same[14]. Table 1 summarizes the thermal quantities (transition temperature and enthalpy (ΔH)) obtained for the DPADPC bilayer membrane.

The thermal behavior of bilayer membranes of ester-liked PC (DPPC) and ether-linked PC (DHPC), which have different linkage of hydrophobic chains to the backbone from DPADPC, is depicted in Figure 6 [37, 38]. The DSC thermogram of the DPPC bilayer membrane in the 1st scan shows three endothermic peaks corresponding to three kinds of phase transition, subtransition from the L_c phase from to the lamellar gel (L_β') phase, pretransition from the L_β' phase to the ripple gel (P_β') phase and main transition from the P_β' phase to the L_α phase, respectively. In the 2nd scan, the subtransition is not observed and the L_β' phase appears as a metastable phase in the low-temperature range because it takes a long time to form the L_c phase [29, 30]. On the other hand, the DSC thermogram of the DHPC bilayer membrane also shows three kinds of phase transition

though, the kinds of transition for the subtransition and the pretransition are different from those of the DPPC bilayer membrane. Since the DHPC bilayer membrane forms the interdigitated structure by only hydration at low temperatures, the hydrated crystal phase is the L_cI phase, not the L_c phase and the L_β' phase is replaced by the $L_\beta I$ phase [36-38]. Accordingly, the subtransition and pretransition of the DHPC bilayer membrane correspond to the transition from the L_cI phase to the $L_\beta I$ phase and that from the $L_\beta I$ phase to the P_β' phase, respectively. Further, all three transitions are observed in the DHPC bilayer membrane irrespective of thermal history of a lipid sample. Regarding the results of cooling scan for the DPPC and DHPC bilayer membranes (data not shown), they reproduce the phase transitions observed in the heating scan although the L_c phase is not observed due to the phase stability (for DPPC) or the existence at lower temperatures (for DHPC).

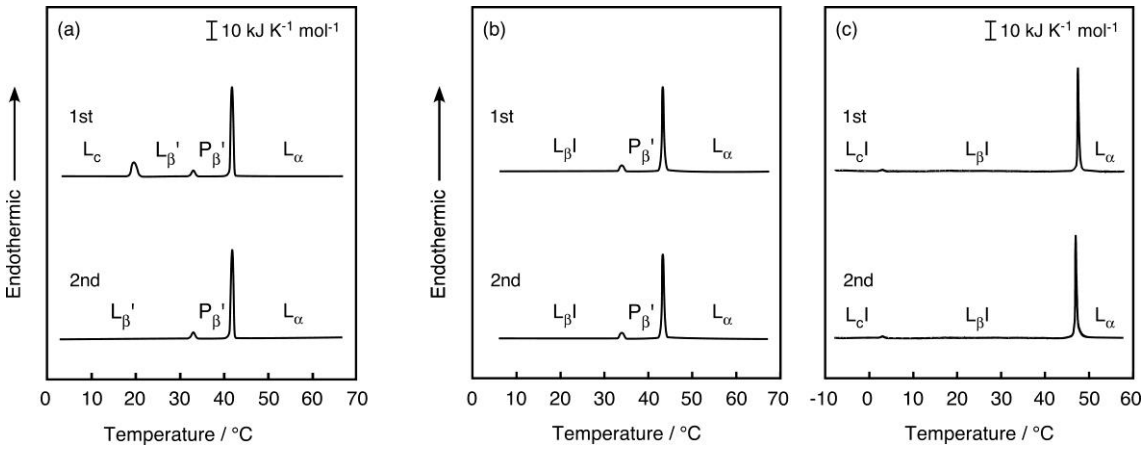

Figure. 6. DSC heating thermograms of annealed bilayer membranes of PC with different chain linkages: (a) DPPC, (b) DHPC (c) DHPC (in 50 wt aqueous EG solution); (1) 1st scan, (2) 2nd scan [35, 36]. Here the DHPC bilayer membrane was also observed in 50 wt aqueous EG solution due to the observation of the L_c phase.

All PC bilayer membranes exhibit three phase states as seen in the DSC thermograms but how to appear the transition peak and stability of each phase are significantly different from one another. It is found from how to appear the transition peak of the gel-phase transitions that the gel phase is completely stable in the DHPC bilayer membrane, partially metastable in the DPPC bilayer membrane and completely metastable in the DPADPC bilayer membrane. And the polymorphism of gel phases is observed in all PC bilayer membranes.

3.3.2. Barotropic phase behavior of DPADPC bilayer membrane:

Figure 7 depicts the results of light-transmittance measurements performed for the DPADPC bilayer membrane under isobaric thermotropic conditions. The transmittance of the dynamically annealed DPADPC bilayer membrane under atmospheric pressure showed a single change: it decreased suddenly at the L_c/L_α-transition temperature (curve 1). The transition temperature increased by applying pressure up to 90 MPa. At higher pressures above 90 MPa, it was frequently observed that the transmittance increases immediately after the decrease (curve 2).

In contrast to this, the transmittance of the non-annealed DPADPC bilayer membrane showed complicated behavior. The transmittance increased sharply at three temperatures of ca. 22, 35 and 41 °C under atmospheric pressure (curve 3). Since we judged the transition at ca. 22 °C as the transition from another gel phase (Gel (x)) to Gel (l) phase because the extent of the increase in transmittance is small. The subsequent stepwise increases in transmittance with increasing temperature are identified from the temperatures of the transition points as the exothermic transition between gel phases (Gel (l)/Gel (h) transition) and main transition (Gel (h)/L_a transition) observed in the DSC

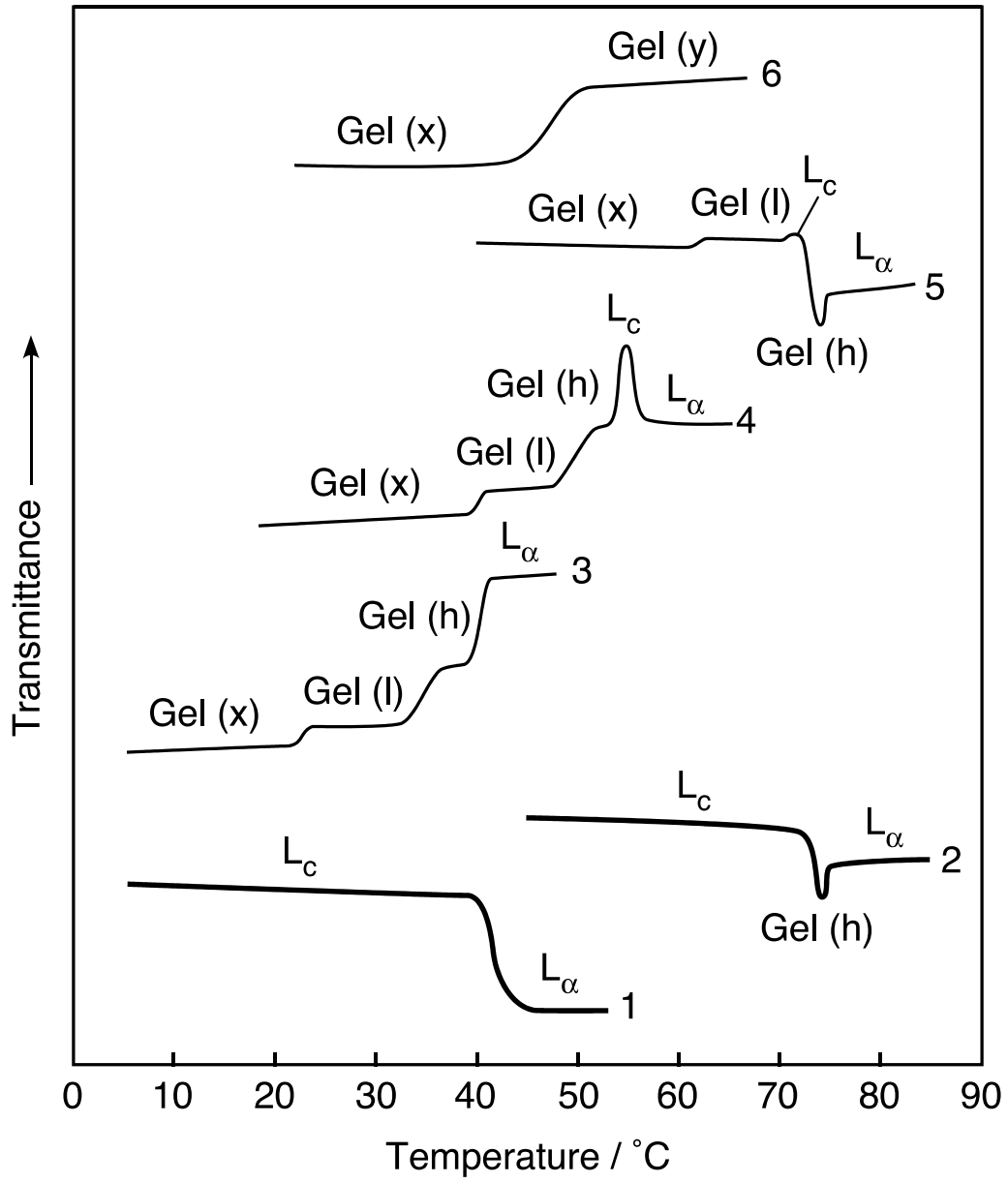

Figure. 7. Typical curves for isobaric thermotropic phase transitions of DPADPC bilayer membrane. Pressure: (a) (1) 0.1 MPa, (2) 150 MPa; (b) (3) 0.1 MPa, (4) 60 MPa, (5) 150 MPa, (6) 170 MPa. Gel (l) and Gel (h) denote low-ordered and high-ordered gel phases, respectively. Gel (x) and Gel (y) are other gel phases observed in this study. Bold and solid lines indicate results of annealing samples and those of non-annealing samples, respectively.

measurements. At 60 MPa, the non-annealed bilayer membrane showed the transmittance increases at three temperatures of ca. 40, 50 and 54 °C but the transmittance conversely decreased at ca. 56 °C (curve 4). Referring to the transmittance behavior under atmospheric pressure, we identified the transitions at ca. 40, 50 and 54 °C as the transition between gel phases (Gel (x)/Gel (l) transition), exothermic transition and main transition, respectively. The decrease in transmittance observed at ca. 56 °C was always observed at higher pressures above 60 MPa. Since this transmittance decrease resembles that of the L_c/L_α transition observed for the annealed bilayer membrane under atmospheric pressure and there is a good correlation between the transition temperature under atmospheric pressure and the extrapolated value from temperatures of the transitions accompanied with the transmittance decrease under high pressure, the author judged that the L_c phase is induced by applying pressure at higher pressures above 60 MPa. At 150 MPa, the transmittance increases by the Gel (x)/Gel (l) transition and exothermic transition were observed at ca. 62 and 70 °C, respectively, however, the transmittance exhibited the different behavior from that observed at 60 MPa in the further heating process. Namely, the transmittance decreased at ca. 72 °C and then increased ca. 75 °C (curve 5) as was observed for the case of the annealed bilayer membrane at higher pressures above 90 MPa.

Furthermore, a broad but relatively large change at ca. 48 °C (curve 6) was observed on the transmittance of non-annealed bilayer membrane at 170 MPa, the change of which showed an increase or decrease in transmittance depending on the measurement-cell type. This fact means that pressure-induced other gel phase (Gel (y)) is induced there. Similar transmittance behavior was also observed in the further higher-pressure region. The author has observed a similar characteristic feature of the transmittance change in the

bilayer interdigitation of diacyl- and dialkyl-phosphatidylcholines with long acyl chains [27, 28, 24, 33]. The feature suggests that the interdigitated gel ($L_{\beta}I$) phase is formed in the higher-pressure region.

3.3.3. Temperature–pressure phase diagram of DPADPC bilayer membrane:

The author constructed the *T–p* phase diagram of the DPADPC bilayer membrane on the basis of the phase-transition data, which were obtained as a function of temperature and pressure from DSC and light-transmittance measurements. The resulting phase diagram is presented in Figure 8. Temperatures of four kinds of phase transitions observed under atmospheric pressure, the transition between gel phases, exothermic transition, main transition and L_c/L_{α} transition, increased by applying pressure. In the phase transitions observed at higher pressures above 150 MPa, temperatures of the higher-temperature transitions above ca. 62 °C increased with increasing pressure while that of the lower-temperature transition below ca. 62 °C conversely decreased with pressure. Regarding the main and L_c/L_{α} transitions, the main transition was located at lower temperatures than the L_c/L_{α} transition under atmospheric pressure, but both main- and L_c/L_{α}-transition curves intersected each other at ca. 85 MPa because the slope (dT/dp) value of the main-transition curve is slightly larger than that of the L_c/L_{α} transition. Therefore, the main transition was located at higher temperatures than the L_c/L_{α} transition at higher pressures above ca. 85 MPa.

The author has revealed thermotropic and barotropic phase behavior of bilayers formed by various phospholipids with different molecular structures by means of their *T–p* phase diagrams. Among the phase diagrams, we have proved that the negative dT/dp

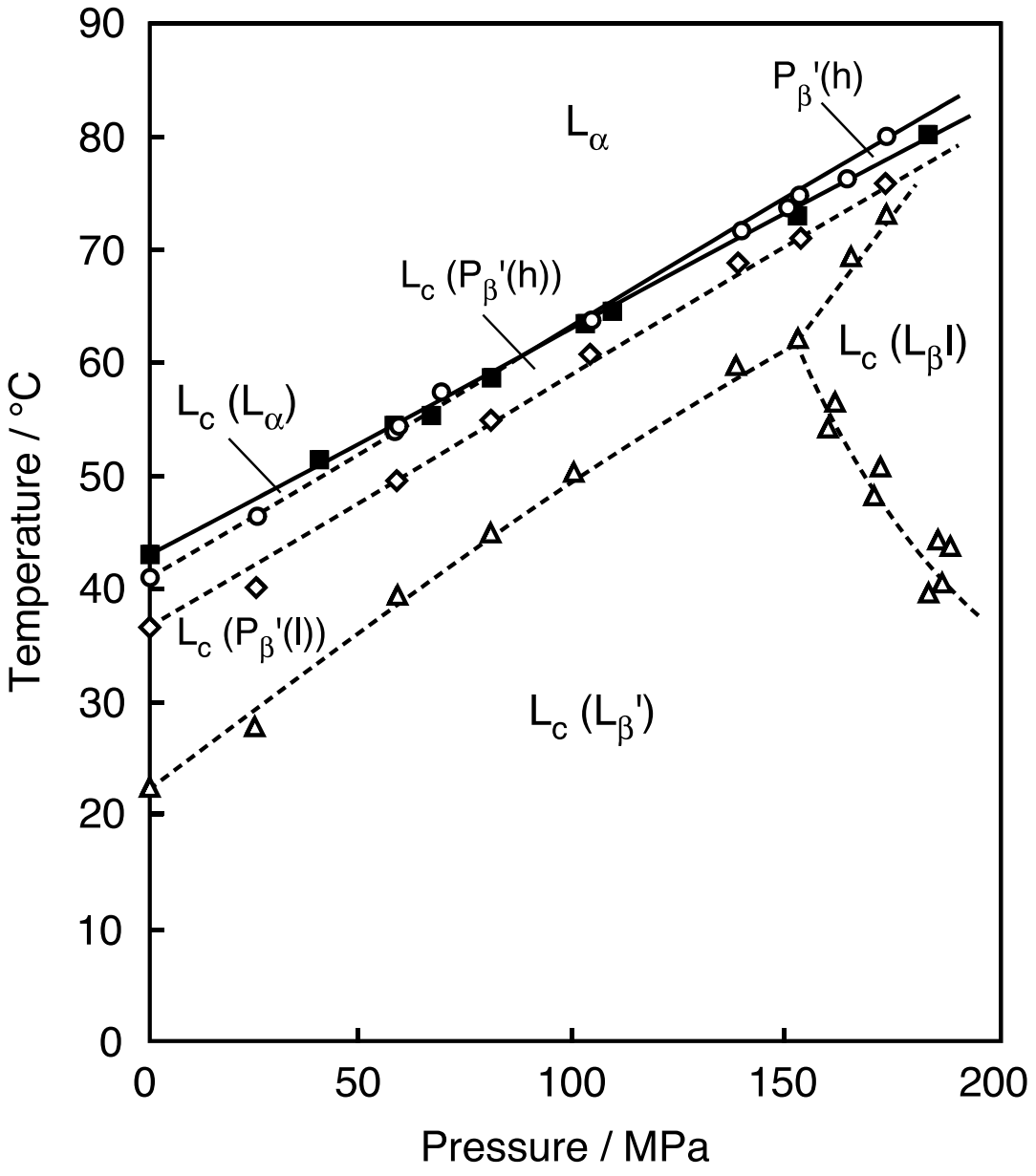

Figure. 8. Temperature-pressure phase diagram of DPADPC bilayer membrane. Phase transitions: (△) $L_{\beta}'/P_{\beta}'(l)$, $L_{\beta}I/P_{\beta}'(l)$ or $L_{\beta}'/L_{\beta}I$ (◇) $P_{\beta}'(l)/P_{\beta}'(h)$, (○) $P_{\beta}'(h)/L_{\alpha}$, (■) L_c/L_{α}. Solid and broken lines indicate phase transitions between stable phases and those between metastable phases, respectively.

value of a phase-transition curve and the intersection of the main- and L_c/L_α-transition curves in the *T–p* diagram are responsible for the bilayer interdigitation of gel phases and the stability change in gel phases between metastable and stable states [24, 33 ,39-41].Taking account of the patterns of *T–p* diagrams, thermal behavior observed in the DSC measurements and thermodynamic properties of phase transition described below into consideration, together with the thermal and structural data in the previous study [18], the author assigned the phases under high pressure. The assigned phases are denoted in the phase diagram of Figure 5. The non-annealed bilayer membrane undergoes two kinds of polymorphic transition between gel phases, that is, the pretransition from the lamellar gel (L_β'), i.e. Gel (x), phase to the low-ordered ripple gel ($P_\beta'(l)$), i.e. Gel (l), phase and the exothermic transition from the $P_\beta'(l)$ phase to the high-ordered ripple gel ($P_\beta'(h)$), i.e. Gel (h), phase and finally the main transition from the $P_\beta'(h)$ phase to the L_α phase, at pressures from 0.1 MPa to ca. 85 MPa. Here the author tentatively assigned the intermediate gel phases below the main-transition temperature as two kinds of the P_β' phases, $P_\beta'(l)$ and $P_\beta'(h)$, deducing the phase behavior of the ester- and ether-linked PC bilayer membranes [35, 36], although the exact phase identification is required by a structural analysis method such as X-ray and neutron scattering under high pressure. Further, the non-bilayer $L_\beta I$, i.e. Gel (y), phase is induced at higher pressures above 150 MPa. On the other hand, the annealed bilayer membrane undergoes the transition from the L_c phase to the L_α phase directly at pressures up to ca. 85 MPa while does the stepwise transitions, the transition from the L_c phase to the $P_\beta'(h)$ phase and transition from the $P_\beta'(h)$ phase to the L_α phase, consecutively at higher pressures above ca. 85 MPa due to the stability change of the $P_\beta'(h)$ phase.

The phase behavior of the DPADPC bilayer membrane was compared with the corresponding ones of chain-linkage isomers, DPPC and DHPC bilayer membranes. The *T*–*p* diagrams of these PC bilayer membranes are demonstrated in Figure 9 [35, 36, 42-44]. The main-transition temperatures under atmospheric pressure and the d*T*/d*p* values of the main-transition curve of these PC bilayer membranes became almost similar to one another, which means the resemblance of the chain-melting transition for the same hydrophobic chains. Concerning the polymorphism of gel phases, although it was observed for all PC bilayer membrane irrespective of the chain-linkage type, the number of gel phases observed increased in the order of DHPC, DPPC and DPADPC bilayer membranes. Here the behavior of the $L_{\beta}I$ phase is interesting. The $L_{\beta}I$ phase of the DHPC bilayer membrane is formed by only hydration under atmospheric pressure while those of the DPPC and DPADPC bilayer membranes are formed under high pressure, and it is understandable that the DPADPC bilayer membrane requires higher pressure to form the phase than the DPPC bilayer membrane. The result indicates that the molecular interaction of PC molecules in the gel phase is strengthened in the order of DHPC, DPPC and DPADPC bilayer membranes. It should be noted that the slope of the $L_{\beta}'/L_{\beta}I$ transition curve of the DPADPC bilayer membrane is steeper (more negative) than that of the DPPC bilayer membrane. Since the ΔH value of the $L_{\beta}'/L_{\beta}I$ transition is positive [45], the negative slope of the transition produces the negative transition-volume (ΔV) value through the Clapeyron equation (cf. Eq. (2)). Thus the ΔV value of the DPADPC bilayer membrane becomes more negative than that of the DPPC bilayer membrane. This fact suggests that the packing of the DPADPC molecules in the gel phases is tighter than that of the DPPC ones. Similar behavior was observed in the salt effect on bilayer interdigitation of a dipalmitoylphosphatidylglycerol bilayer membrane [46]. In addition

to the gel-phase behavior, there was a pronounced difference in the transition related to the L_c phase among them. The transition temperature increased by about 20 °C in the order of DHPC, DPPC and DPADPC membranes. The curve of the transition related to the L_c phase was located at lower temperatures than the main transition-curve in the DPPC and DHPC bilayer membranes, whereas both curves intersected at ca. 85 MPa in the DPADPC bilayer membrane because the curve of the transition related to the L_c phase greatly shifts to the high-temperature region and both curves come close to each other. The author can say from this result that the molecular interaction of PC molecules in the L_c phase is also enhanced in the order of DHPC, DPPC and DPADPC bilayer membranes.

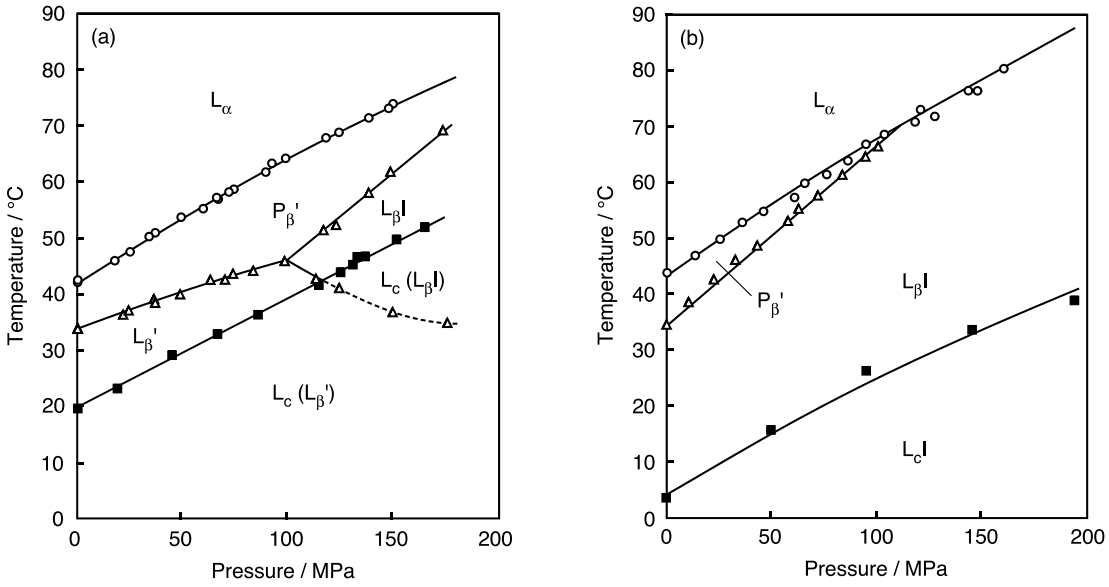

Figure. 9. Temperature–pressure phase diagrams of bilayer membranes of PC with different chain linkages: (a) DPPC, (b) DHPC. Phase transitions: (■) $L_c/L\beta'$ or $L_cI/L\beta I$, (△) $L\beta'/P\beta'$, $L\beta I/P\beta'$ or $L\beta'/L\beta I$, (○) $P\beta'/L\alpha$. Solid and broken lines indicate phase transitions between stable phases and those between metastable phases, respectively.

3.3.4. Thermodynamic properties of phase transitions for DPADPC bilayer membrane:

Thermodynamic properties of the DPADPC bilayer membrane under atmospheric pressure, which were determined from the thermal and pressure measurements, are listed in Table 1. The value of transition entropy (ΔS) was obtained with the ΔH value from DSC measurements and the equation,

$$\Delta S = \Delta H/T \quad (1)$$

And the ΔV value was calculated by the Clapeyron equation with the ΔH value.

$$\Delta V = \Delta H(\mathrm{d}T/\mathrm{d}p)T \quad (2)$$

Here the corresponding results of the DPPC and DHPC bilayer membranes are also included in the table.

The thermodynamic quantities of the L_c/L_α and high-ordered gel/L_α transitions for the DPADPC bilayer membrane had both relatively large values of about 50 – 60 kJ mol^{-1}. Regarding the values of the non-annealed bilayer membrane, when the author estimated the total thermodynamic-quantity values from the low-ordered gel phase to the L_α phase (ΔH = 39.4 kJ mol^{-1}, ΔS = 125 K^{-1} kJ mol^{-1}, ΔV = 27.3 cm^3 mol^{-1}) and compared them with those of main (gel/L_α) transition of the DPPC and DHPC bilayer membranes, the values of the three PC bilayer membranes are roughly comparable to one another. In addition to this fact, the temperatures and dT/dp values of the main transition for these PC bilayer membranes also resembled one another. These thermodynamic properties support that the phase at a low temperature of the non-annealed DPADPC bilayer membrane is the gel phase, not the L_c phase, and describe that the three PC bilayer membranes undergo the similar chain-melting transition irrespective of the difference in chain-linkage type.

On the other hand, the transition related to the L_c phase of the three PC bilayer membranes formed a striking contrast to one another. The DPADPC bilayer membrane directly undergoes the transition from the L_c phase to the L_α phase as mentioned above, but the DPPC and DHPC bilayer membranes undergo from the hydrated crystal (L_c or L_cI) phase to the gel (L_β' or $L_\beta I$) phase, and subsequently the transition from the gel phase to the L_α phase because the gel phase exists as a stable phase under atmospheric pressure. Taking these facts into consideration and evaluating the ΔH and ΔV values of the transition from the hydrated crystal phase to the L_α phase of the DPPC and DHPC bilayer membranes, the author obtained values of 67.3 kJ mol^{-1} and 43.5 cm^3 mol^{-1} for the DPPC bilayer membrane and of ca. 40 kJ mol^{-1} and ca. 31 cm^3 mol^{-1} for the DHPC bilayer membrane. The thermodynamic quantity values of the DPADPC bilayer membrane are almost comparable to those of the DPPC bilayer membrane, indicating that the L_c phase of the DPADPC bilayer membrane as stable as that of the DPPC bilayer membrane. However, the formation of the L_c phase for the DPADPC bilayer membrane occurs with rapid kinetics [44] and it is a racemic compound. It has been reported that the formation of the L_c phase for the DPPC bilayer membrane is the superlattice formation with slow kinetics [47, 48] and the bilayer membrane of its racemic compound hardly forms the L_c phase although it exhibits almost the same main transition as the corresponding optical isomers [49]. These facts suggest that the bilayer membrane of DPADPC forms the more stable L_c phase than that of DPPC and shows tight molecular packing irrespective of its racemic form due to the enhanced molecular interaction.

Table 1. Thermodynamic properties for the bilayer phase transitions of PCs with different chain linkages

Lipid	P. T.	T	dT/dp	ΔH	ΔS	ΔV
		(°C)	(K MPa^{-1})	(kJ mol^{-1})	(J K^{-1} mol^{-1})	(cm^3 mol^{-1})
DPADPC	L_β'/P_β'(l)	22.2	0.27	—	—	—
	P_β'(l)/P_β'(h)	34.1	0.23	–8.0	–26	–6.0
	P_β'(h)/L_α	40.6	0.22	47.4	151	33.3
	L_c/L_α	41.4	0.20	61.0	194	38.8
DPPC	L_c/L_β'	21.5	0.18	26.3	89	16.1
	L_β'/P_β'	34.3	0.13	4.6	15	2.0
	P_β'/L_α	42.0	0.22	36.4	116	25.4
DHPC	$L_cI/L_\beta I$	2.8 [a]	0.20	0.7 [a]	2.5 [a]	—
	$L_\beta I/P_\beta'$	34.2	0.31	5.3	17	5.3
	P_β'/L_α	43.6	0.24	33.7	106	25.3

[a]Results obtained in 50 wt% aqueous ethylene glycol solution.

3.3.5. Motility of the PC molecules in the bilayer membrane:

The effect of chain-linkage type on the interaction among PC molecules in the bilayer membranes from NMR measurements was further examined. Here the author evaluated the motility of the PC molecules by use of ^{13}C-NMR spectra of three PC bilayer membranes [50]. Since the peak intensity of ^{13}C-NMR spectra of the DPADPC bilayer membrane obtained in this study is significantly lower than the DPPC and DHPC bilayer membranes, the motility in each PC molecule in the bilayer membrane was evaluated by the half-value width ($\nu_{1/2}$) of a peak spectrum (the peak width at half height from the maximum value of the spectrum) rather than the relaxation time [51, 52] which is frequently used as a measure of molecular motility and is inversely proportional to the $\nu_{1/2}$ value [50].

The ^{13}C-NMR spectra of the DPADPC bilayer membrane at various temperatures are demonstrated in Figure 10 together with the corresponding ones of the DPPC and DHPC bilayer membranes. Here the assignment of each peak is given in Table 2 [52]. Since the peaks except that of the choline methyl group in the PC molecules almost disappear in the low-temperature region below the main-transition temperature, the motility of the PC molecule was evaluated from the behavior of the choline methyl group in this study. The $\nu_{1/2}$ value obtained for each PC bilayer membrane is plotted against temperature in Figure 11. The measurements were performed in the cooling process in order to take the motility of the L_α phase of each lipid as the standard. The $\nu_{1/2}$ value in all PC bilayer membranes increased sharply in the vicinity of the main-transition temperature with decreasing temperature, indicating that the motility is significantly suppressed as the L_α phase changes to the gel phase. In the L_α phase, both DPPC and DHPC bilayer membranes took almost the same $\nu_{1/2}$ values, by contrast, the DPADPC

bilayer membrane did a much larger value as seen in Figure 11(a). On the other hand, there was a clear difference in the $\nu_{1/2}$ value between the DHPC and DPPC bilayer membranes in the gel phase, and the value of the DHPC bilayer membrane became smaller than that of the DPPC bilayer membrane (Figure 11(b)). For the DPADPC bilayer membrane, the $\nu_{1/2}$ value was also much larger than those of both bilayer membranes in the gel phase as the case in the L_α phase. Furthermore, a significant change was neither observed in the $\nu_{1/2}$ value near the pretransition temperature of the DHPC and DPPC bilayer membranes nor near the exothermic transition of the DPADPC membrane, which were observed in the DSC measurements.

Table 2. Assignment of ^{13}C resonances of DPPC in the bilayer membrane

Resonance	Chemical shift, ppm
Palmitoyl methyl	14
First methylene	22
Second methylene	25
Bulk methylene	30
Methylene	32, 34
Choline methyl	54
Choline methylene	59
Glycerol methylene	63, 63.6
Choline methylene	66
Glycerol methylene	70
Carbonyl	173

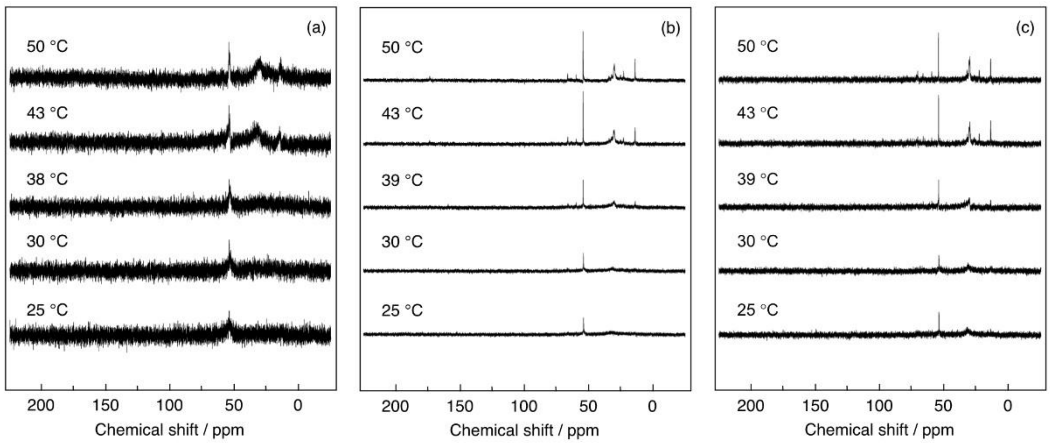

Figure. 10. ^{13}C-NMR spectra of bilayer membranes of PC with different chain linkages: (a) DPADPC, (b) DPPC, (c) DHPC. Here the ordinate of results of the DPADPC bilayer membrane is magnified by 10 times.

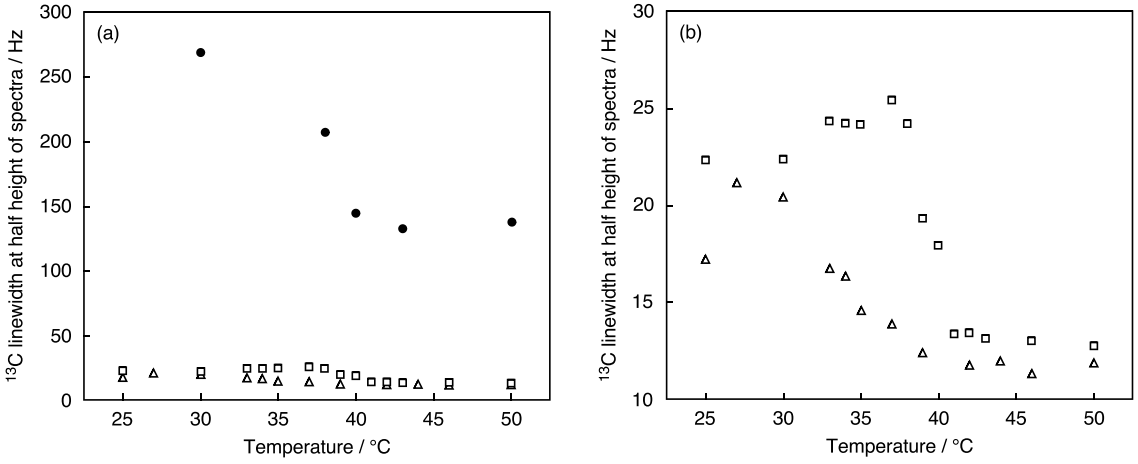

Figure. 11. Temperature dependence of ^{13}C linewidth at half height of spectra for choline methyl group bilayer membranes of PC with different chain linkages under atmospheric pressure: (a) (●) DPADPC, (□) DPPC, (△) DHPC; (b) Magnification of low-value region.

The above results imply that the motility of both DHPC and the DPPC molecules in the L_α phase is similar to each other while the DPPC molecule in the gel phase is restricted as compared with the DHPC one. In our previous paper [28, 36], the author has thermodynamically revealed that the interaction of ether-linked PC molecules in the gel phase is weaker than that of ester-linked PC ones, and the present result is well consistent with this fact. On the other hand, it is understandable in the DPADPC bilayer membrane that the motility of choline methyl group is extremely reduced in comparison with those of the DHPC and DPPC bilayer membranes in both the L_α and gel phases: they undergo significant molecular restriction. It has been reported [10, 14, 18, 19] that amide bonds of a PC molecule in bilayer membranes of amide-linked PC such as DPADPC and its homologs have an ability to form intermolecular hydrogen bonds between adjacent molecules. Significant molecular restriction observed in the DPADPC bilayer membrane may be attributable to the strong backbone interaction acting in the bilayer membrane. Therefore, it can be concluded that the interaction in these PC bilayer membrane increases in the order of DHPC, DPPC and DPADPC as is given in Figure 12. The order of this interaction in the bilayer distinctly explains the characteristic phase behavior emerged on the phase diagram of respective PC bilayer membranes, such as the contrastive L_c phase-formation, gel-phase polymorphism and bilayer interdigitation.

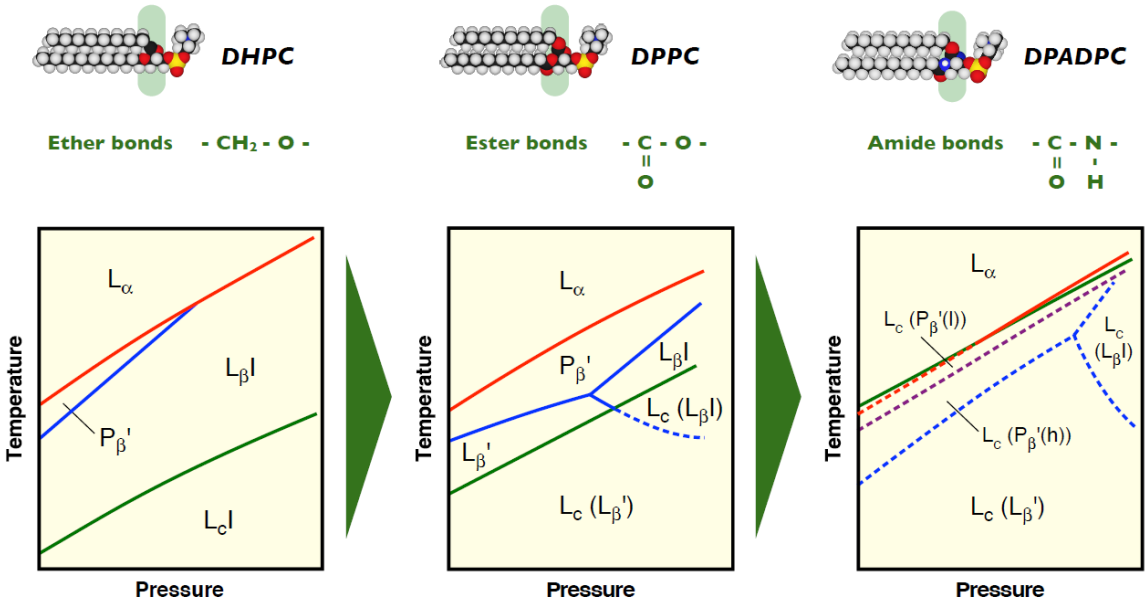

Figure. 12. The lipid interaction in the bilayer membrane increases in the order of ether-linked PC (DHPC), ester-linked PC (DPPC) and amide-linked PC (DPADPC).

Chapter 4.

Comprehensive Summary

The diversity of lipid molecules is produced by numerous combinations of two hydrophobic chains and a hydrophilic polar head group, which are variable module structures, respectively. On the other hand, there is another resource of the diversity in lipids but not in normal surfactants. That is, linkage types connecting both modules are also variable. There exist three linkage types in lipids of biological membranes: ester, ether and amide linkages. The ester- and ether-linkages are found in lipids of biological membranes for almost all living organisms while the amide-linkage is found in limited lipids of higher organisms like sphingophospholipids of eukaryotes. In this study, the author focuses on the effect of the linkage type on bilayer properties of phospholipids.

In the chapter 2, the author synthesized racemic amide-linked unnatural phospholipids with different chain lengths, *rac*-DLADPC, *rac*-DMADPC, *rac*-DPADPC, and *rac*-DSADPC. And subsequently, pure optical isomers of DMADPC and DPADPC, that is, *R*-DMADPC and *R*-DPADPC were also synthesized. Here we selected a *rac*-DPADPC among these synthesized amide-linked PCs for experiments of bilayer properties PCs with different chain-linkages by taking account of our previous results of other PCs and the priority order among the amide-linked PCs.

Chapter 3 described the behavior of the bilayer membrane formed by *rac*-DPADPC. The DPADPC bilayer membrane underwent phase transitions among the L_c, gel and L_α phases specifically depending on the thermal history of the lipid sample. Comparing the bilayer properties of DPADPC with those of chain-linkage isomers DPPC and DHPC,

the thermodynamic quantities of the chain-melting transition between the gel and L_α phases were almost similar for all the PC bilayers. However, in the condensed phases like the L_c and gel phases, all the PC bilayers exhibited definite different behavior due to the difference in chain-linkage type, which indicates that the DPADPC bilayer membrane produces the tightest phase states of all the PC bilayers. Moreover, the motility of the DPADPC molecules in the bilayer membrane are significantly restrained in both gel and L_α phases as compared to those of the DPPC and DHPC bilayer membranes, suggesting that there exits strong molecular interaction between the chain-linkage portions arising from the intermolecular hydrogen bonding. It turned out that the introduction of amide bonds to the lipid backbone brings about the marked reinforcement of tighter membrane packing than that of ester bonds and ether bonds.

The phospholipid used in the membrane properties of this thesis is an unnatural PC with two symmetric hydrophobic chains and also a racemic compound. Biological membranes are generally occupied with asymmetric phospholipids with different hydrophobic chains and/or different chain linkages as sphingophospholipids. As a next step in the future, by extending similar studies on hydrophobic chain analogs and optical isomers (*R*-form) of amide-linked PCs synthesized in this study and on the positional and another optical isomers (*S*-form) and by making comprehensive comparison of the bilayer properties, it is expected that the effect of chain-linkage type on membrane states of phospholipids will be able to further make clear.

Acknowledgements

The present dissertation was written on the basis of the research carried out at the laboratory of A1 and/or C1 research group, Biological Science and Technology, Life and Materials Systems Engineering, Graduate School of Advanced Technology and Science, Tokushima University, from 2016 to 2022 under the direction of Professor Hitoshi Matsuki, Division of Bioscience and Bioindustry, Graduate School of Technology, Industrial and Social Sciences, Tokushima University, to whom the author wishes to express his sincere gratitude for the continuous guidance and encouragement.

The author would like to express his heartful gratitude to Associate Professors Nobutake Tamai and Masaki Goto, Division of Bioscience and Bioindustry, Graduate School of Technology, Industrial and Social Sciences, Tokushima University, for their cooperation in submitting my paper to academic journals and collaboration on thermal and high-pressure experiments.

The author is also so grateful to Professor Mikito Yasuzawa and Assistant Professor Masashi Kurashina, Division of Science and Technology, Graduate School of Technology, Industrial and Social Sciences, Tokushima University, for teaching me various techniques of organic synthesis.

Thanks are due to Ms. Zhao Yumeng for her English advice and encouragement, and also due to all past and current members of the laboratory of A1 and/or C1 research group.

References

1. W. Stillwell: An Introduction to Biological Membranes (Academic Press, San Diego, 2013).

2. L.K. Buehler, in: Cell Membranes, Garland Science, Taylor & Francis Group, New York, 2016, pp. 86–90.

3. E. Gorter and F. Grendel."On bimolecular layers of lipids on the chromocytes of the blood." *Journal of Experimental Medicine*, 41 (1925) 439-443.

4. J. F. Danielli and H. Davson."A contribution to the theory of permeability of thin films." *Journal of Cellular and Comparative Physiology,* 5 (1935) 495-508.

5. S. J. Singer, G. L. Nicolson, The fluid mosaic model of the structure of cell membranes, *Science* 175 (1972) 720–731.

6. K. Simons, E. Ikonen, Functional rafts in cell, *Nature* 387 (1997) 569–572.

7. A. Rietveld, K. Simons, The differential miscibility of lipids as the basis for the formation functional membrane rafts, *Biochim. Biophys. Acta* 1376 (1998) 467–479.

8. K. Simons, E. Ikonen, How cells handle cholesterol, *Science* 290 (2000) 1721–1726.

9. R. N. A. H. Lewis, R. N. McElhaney: in The Structure of Biological Membranes, ed. P. L. Yeagle (CRC press, London, 2012), Chap. 4, pp. 23-29.

10. J. Sunamoto, M. Goto, K. Iwamoto, H. Kondo, T. Sato, Synthesis and characterization of 1,2-dimyristoylamido-1,2-deoxyphosphatidylcholine as an artificial boundary lipid, *Biochim. Biophys. Acta* 1024 (1990) 209–219.

11. J. Sunamoto, K. Nagai, M. Goto, B. Lindman, Deuterium nuclear magnetic resonance studies on the interaction of glycophorin with 1,2- dimyristoylamido-1,2-deoxyphosphatidylcholine, *Biochim. Biophys. Acta* 1024 (1990) 220–226.

12. M. Goto, J. Sunamoto, Effect of artificial boundary lipid on the membrane dynamics of human glycophorin-containing liposome, *Bull. Chem. Soc. Jpn*. 65 (1992) 3331–3334.

13. Z. Zhou, Y. Okumura, J. Sunamoto, NMR study of choline methyl group of phospholipids, *Proc. Jpn. Acad.* 72B (1996) 23–27.

14. H. Takahashi, Y. Okumura, J. Sunamoto, Structure and thermal history dependant phase behavior of hydrated synthetic sphingomyelin analogue: 1,2-dimyristamido-1,2-deoxyphosphatidylcholine, *Biochim. Biophys. Acta* 1713 (2005) 40–50.

15. I. A. Fedotenko, C. Stefaniu, G. Brezesinski, A. Zumbuehl, Monolayer properties of 1,3-diamidophospholipids, *Langmuir* 29 (2013) 9428−9435.

16. A. Weinberger, R. Tanasescu, C. Stefaniu, I. A. Fedotenko, F. Favarger, T. Ishikawa, G. Brezesinski, C. M. Marques, A. Zumbuehl, Bilayer properties of 1,3-diamidophospholipids, *Langmuir* 31 (2015) 1879−1884.

17. R. Tanasescu, M. A. Lanz, D. Mueller, S. Tassler, T. Ishikawa, R. Reiter, G. Brezesinski, A. Zumbuehl, Vesicle origami and the influence of cholesterol on lipid packing, *Langmuir* 32 (2016) 4896−4903.

18. F. Neuhaus; D. Mueller, R. Tanasescu; S. Balog; T. Ishikawa; G. Brezesinski; A. Zumbuehl, Vesicle origami: cuboid phospholipid vesicles formed by template-free self-assembly, *Angew. Chem. Int. Ed*., 129 (2017) 6615−6618.

19. A. Zumbuehl, Artificial phospholipids and their vesicle, *Langmuir*, 35 (2019) 10223−10232.

20. S. Matviykiv, H. Deyhle, J. Kohlbrecher, F. Neuhaus, A. Zumbuehl, B. Müller, Small-angle neutron scattering study of temperature-induced structural changes in liposomes, *Langmuir* 35 (2019) 11210−11216.

21. M. Savva, P. Chen, A. Aljaberi, B. Selvi, M. Spelios, In vitro lipofection with novel asymmetric series of 1,2-dialkoylamidopropane-based cytofectins containing single symmetric bis-(2-dimethylaminoethane) polar headgroups, *Bioconjug. Chem.* 16

(2005) 1411−1422.

22. H.S. Byun, R. Bittman, Efficient stereospecific synthesis of diamide analogs of phosphatidylcholine starting from 1-(4'-methoxyphenyl)-sn-glycerol, *J. Org. Chem*. 61 (1996) 8706−8708

23. H. Matsuki, M. Goto, K. Tada, N. Tamai, Thermotropic and barotropic phase behavior of phosphatidylcholine bilayers, *Int. J. Mol. Sci*. 14 (2013) 2282–2302.

24. M. Goto, T. Endo, T. Yano, N. Tamai, J. Kohlbrecher, H. Matsuki, Comprehensive characterization of temperature- and pressure-induced phase transitions for saturated phosphatidylcholines containing longer chain homologs, Colloids Surf. B: Biointerf. 128 (2015) 389–397.

25. H. Matsuki, How do membranes respond to pressure?, in: K. Akasaka, H. Matsuki (Eds.), High Pressure Bioscience, Basic Concepts, Applications and Frontiers, Chapter 16, Springer, Dordrecht, 2015, pp. 321–343.

26. H. Matsuki, M. Goto, N. Tamai, Membrane states of saturated glycerophospholipids: a thermodynamic study of bilayer phase transitions, Chem. Pharm. Bull. 67 (2019) 300–307.

27. S. Maruyama, H. Matsuki, H. Ichimori, S. Kaneshina, Thermotropic and barotropic phase behavior of dihexadecylphosphatidylcholine bilayer membrane, *Chemistry and Physics of Lipids*, 82 (1996) 125–132.

28. H. Matsuki, E. Miyazaki, F. Sakano, N. Tamai, S. Kaneshina, Thermotropic and barotropic phase transitions in bilayer membranes of ether-linked phospholipids with varying alkyl chain lengths. *Biochim Biophys Acta* 1768, (2007) 479–489.

29. M. Goto, T. Endo, T. Yano, N. Tamai, J. Kohlbrecher, H. Matsuki, Comprehensive characterization of temperature- and pressure-induced bilayer phase transitions for saturated phosphatidylcholines containing longer chain homologs, *Colloids Surf. B: Biointerf.* 2015, 128, 389-397.

30. R.N.A.H. Lewis, N. Mak, R.N. McElhaney, A differential scanning calorimetric

study of the thermotropic phase behavior of model membranes composed of phosphatidylcholines containing linear saturated fatty acid chains, *Biochemistry*, 26 (1987) 6118–6126.

31. H. Aoki, M. Kodama, Calorimetric investigation of the behavior of interlamellar water in phospholipid-water systems, *Thermochim. Acta* 308 (1998) 77–83.

32. M. Kodama, H. Kato, H. Aoki, Comparison of differently bound molecules in the gel and subgel phases of a phospholipid bilayer system, *J. Therm. Anal. Cal*. 64 (2001) 219–230.

33. H. Ichimori, T. Hata, H. Matsuki, S. Kaneshina, Barotropic phase transitions and pressure-induced interdigitation on bilayer membranes of phospholipids with varying acyl-chain lengths, *Biochim. Biophys. Acta* 1414 (1998) 165–174.

34. K. Sato, Crystallization behaviour of fats and lipids – a review, *Chem. Eng. Sci.* 56 (2001) 2255–2265.

35. M. Kusube, H. Matsuki, S. Kaneshina, Thermotropic and barotropic phase transitions of N-methylated dipalmitoylphosphatidylethanolamine bilayers, *Biochim. Biophys. Acta* 1668 (2005) 25–32.

36. M. Goto, H. Sawaguchi, N. Tamai, H. Matsuki, Subgel-phase formation of membranes of ether-linked phosphatidylcholines, *Chem. Phys. Lipids*, 239 (2021) 105119-1-105119-8.

37. J. T. Kim, J. Mattai, G. G. Shipley, Gel phase polymorphism in ether-linked dihexadecylphosphatidylcholine bilayers, *Biochemistry* 26 (1987) 6592–6598.

38. P. Laggner, K. Lohner, G. Degovics, K. Müller, A. Schuster, Structure and thermodynamics of the dihexadecylphosphatidylcholine-water system, *Chem. Phys. Lipids* 44 (1987) 31–60.

39. S. Kaneshina, H. Ichimori, T. Hata, H. Matsuki, Barotropic phase transitions of dioleoylphosphatidylcholine and stearoyl-oleoylphosphatidylcholine bilayer membranes, *Biochim. Biophys. Acta* 1374 (1998) 1–8.

40. M. Kusube, M. Goto, N. Tamai, H. Matsuki, S. Kaneshina, Bilayer phase transitions of N-methylated dioleoylphosphatidylethanolamines under high pressure, *Chem. Phys. Lipids* 142 (2006) 94–102.

41. H. Matsuki, S. Endo, R. Sueyoshi, M. Goto, N, Tamai, S. Kaneshina, Thermotropic and barotropic phase transitions on diacylphosphatidylethanolamine bilayer membranes, *Biochim. Biophys. Acta* 1859 (2017) 1222–1232.

42. M. J. Ruocco and G. G. Shipley, Characterization of the sub-transition of hydrated dipalmitoylphosphatidylcholine bilayers, *Biochim. Biophys. Acta* 1982, 691, 320.

43. J. Stümpel, H. Eibl, A. Nicksch, X-ray analysis and calorimetry on phosphatidylcholine model membranes. The influence of length and position of acyl chains upon structure and phase behavior, *Biochim Biophys. Acta* 1983, 727, 246-254.

44. M. Kodama, Phase transition phenomena induced by the successive appearances of new types of aggregation states of water molecules in the "l-dipalmitoylphosphatidylcholine-water" system, *Thermochim. Acta* 1986, 109, 81-89.

45. F. Zhang, E. S. Rowe, Titration calorimetric and differential scanning calorimetric studies of the interactions of n-butanol with several phases of dipalmitoylphosphatidylcholine, *Biochemistry* 31 (1992), 2005–2011.

46. M. Goto, H. Okamoto, N. Tamai, K. Fukada, H. Matsuki, Salt effect on bilayer phase transitions of dipalmitoylphosphatidylglycerol in saline water under high pressure, *High Pressure Res*. 39 (2019) 238–247.

47. J. Katsaras, V. A. Raghunathan, E. J. Dufourc, J. Dufourcq, Evidence for a two-dimensional molecular lattice in subgel phase DPPC bilayers, *Biochemistry* 34 (1995) 4684–4688.

48. V. A. Raghunathan, J. Katsaras, Structure of the Lc' phase in a hydrated lipid multilamellar system, *Phys. Rev. Lett.* 74 (1995) 4456–4459.

49. M. Kodama, H. Hashigami, S. Seki, Static and dynamic calorimetric studies on the three kinds of phase transition in the systems of L- and DL-dipalmitoylphosphatidylcholine/water, *Biochim. Biophys. Acta* 814 (1985) 300–306.

50. T. C. Farrar, E. D. Becker, In Pulse and Fourier Transform NMR: Introduction to Theory and Methods, Academic Press, New York, 1971, Chapter 1, pp. 1–17.

51. A. B. Kohn, S. E. Schullery, Dipalmitoylphosphatidylcholine-palmitic acid phase diagram studied by 13C nuclear magnetic resonance, *Chem. Phys. Lipids,* 37 (1985) 143–153.

52. J. Jonas, C.-L. Xie, A. Jonas, P. J. Grandinetti, D. Campbell, D. Driscoll, High-resolution 13C NMR study of pressure effects on the main phase transition in L-α-dipalmitoyl phosphatidylcholine vesicles, *Pro. Natl. Acad. Sci. USA*, 85 (1988) 4115–4117.